cell lung cancer to gefitinib. N Engl J Med 2004;350:2129–39.
[2] Paez JG, Janne PA, Lee JC, Tracy S, Greulich H, Gabriel S, et al. EGFR mutations in lung cancer: correlation with clinical response to gefitinib therapy. Science 2004;304:1497–500.
[3] Kobayashi S, Boggon TJ, Dayaram T, Janne PA, Kocher O, Meyerson M, et al. EGFR mutation and resistance of non-small-cell lung cancer to gefitinib. N Engl J Med 2005;352:786–92.
[4] Koizumi F, Shimoyama T, Taguchi F, Saijo N, Nishio K, Kanzawa F, et al. Establishment of a human non-small cell lung cancer cell line resistant to gefitinib Synergistic interaction between the EGFR tyrosine kinase inhibitor gefitinib ("Iressa") and the DNA topoisomerase I inhibitor CPT-11 (irinotecan) in human colorectal cancer cells. Int J Cancer 2005;116:36–44.
[5] Naruse I, Ohmori T, Ao Y, Fukumoto H, Kuroki T, Mori M, et al. Antitumor activity of the selective epidermal growth factor receptor-tyrosine kinase inhibitor (EGFR-TKI) Iressa (ZD1839) in an EGFR-expressing multidrug-resistant cell line in vitro and in vivo. Int J Cancer 2002;98:310–5.
[6] Kanzawa F, Akiyama Y, Saijo N, Nishio K. In vitro effects of combinations of cis-amminedichloro (2-methylpyridine) platinum(II) (ZD0473) with other novel anticancer drugs on the growth of SBC-3, a human small cell lung cancer cell line. Lung Cancer 2003;40:325–32.
[7] Chou TC, Talalay P. Quantitative analysis of dose-effect relationships: the combined effects of multiple drugs or enzyme inhibitors. Adv Enzyme Regul 1984;22:27–55.
[8] Ciardiello F, Caputo R, Bianco R, Damiano V, Pomatico G, De Placido S, et al. Antitumor effect and potentiation of cytotoxic drugs activity in human cancer cells by ZD-1839 (Iressa), an epidermal growth factor receptor-selective tyrosine kinase inhibitor. Clin Cancer Res 2000;6:2053–63.
[9] Sirotnak FM, Zakowski MF, Miller VA, Scher HI, Kris MG. Efficacy of cytotoxic agents against human tumor xenografts is markedly enhanced by coadministration of ZD1839 (Iressa), an inhibitor of EGFR tyrosine kinase. Clin Cancer Res 2000; 6:4885–92.
[10] Giaccone G, Herbst RS, Manegold C, Scagliotti G, Rosell R, Miller V, et al. Gefitinib in combination with gemcitabine and cisplatin in advanced non-small-cell lung cancer: a phase III trial—INTACT 1. J Clin Oncol 2004;22:777–84.
[11] Herbst RS, Giaccone G, Schiller JH, Natale RB, Miller V, Manegold C, et al. Gefitinib in combination with paclitaxel and carboplatin in advanced non-small-cell lung cancer: a phase III trial—INTACT 2. J Clin Oncol 2004;22:785–94.
[12] Taguchi F, Koh Y, Koizumi F, Tamura T, Saijo N, Nishio K. Anticancer effects of ZD6474, a VEGF receptor tyrosine kinase inhibitor, in gefitinib ("Iressa")-sensitive and resistant xenograft models. Cancer Sci 2004;95:984–9.
[13] Arao T, Fukumoto H, Takeda M, Tamura T, Saijo N, Nishio K. Small in-frame deletion in the epidermal growth factor receptor as a target for ZD6474. Cancer Res 2004;64:9101–4.
[14] Koizumi F, Kanzawa F, Ueda Y, Koh Y, Tsukiyama S, Taguchi F, et al. Synergistic interaction between the EGFR tyrosine kinase inhibitor gefitinib ("Iressa") and the DNA topoisomerase I inhibitor CPT-11 (irinotecan) in human colorectal cancer cells. Int J Cancer 2004;108:464–72.
[15] Barber TD, Vogelstein B, Kinzler KW, Velculescu VE. Somatic mutations of EGFR in colorectal cancers and glioblastomas. N Engl J Med 2004;351:2883.
[16] van Ark-Otte J, Kedde MA, van der Vijgh WJ, Dingemans AM, Jansen WJ, Pinedo HM, et al. Determinants of CPT-11 and SN-38 activities in human lung cancer cells. Br J Cancer 1998;77:2171–6.
[17] Park JK, Lee SH, Kang JH, Nishio K, Saijo N, Kuh HJ. Synergistic interaction between gefitinib (Iressa ZD1839) and paclitaxel against human gastric carcinoma cells. Anticancer Drugs 2004;15:809–18.

The Pharmacogenomics Journal (2006), 1–9
© 2006 Nature Publishing Group All rights reserved 1470-269X/06 $30.00
www.nature.com/tpj

ORIGINAL ARTICLE

Reference profiling of the genomic response induced by an antimicrotubule agent, TZT-1027 (Soblidotin), *in vitro*

T Shimoyama[1,2], T Hamano[1], T Natsume[1], F Koizumi[1], K Kiura[2], M Tanimoto[2] and K Nishio[1,3]

[1]*Shien-Lab and Medical Oncology, National Cancer Center Hospital, Chuo-ku, Tokyo, Japan;* [2]*Department of Medicine II, Okayama University Medical School, Shikata-cho, Okayama, Japan and* [3]*Pharmacology Division, National Cancer Center Research Institution, Chuo-ku, Tokyo, Japan*

Correspondence:
Dr K Nishio, Shien-Lab, National Cancer Center Hospital, 5-1-1 Tsukiji, Chuo-ku, Tokyo 104-0045, Japan.
E-mail: knishio@gan2.res.ncc.go.jp

Received 24 October 2005; revised 20 January 2006; accepted 16 February 2006

TZT-1027 is an antimicrotubule agent targeting beta-tubulin that is undergoing clinical development. The genomic response of cancer cells to TZT-1027 was profiled to evaluate its biochemical activity. A lung cancer cell line, PC-14, was exposed to antimicrotubule agents including dolastatins, *Vinca* alkaloids and taxanes at an equivalent toxicity level. Alterations in the TZT-1027-induced gene expression of ~600 genes were then examined using microarray technology and the resulting gene profiles were compared with those for cells exposed to the other antimicrotubule agents. A principle component analysis using the whole gene set demonstrated that TZT-1027 produced similar gene profiles to those produced by dolastatin 10, but that these gene profiles differed from those produced by other agents. The agents were classified according to their induced genomic response in a molecular structure-dependent manner. Genes whose expression profiles differed according to drug class included intermediate filaments, extracellular matrix protein and Rho regulatory genes that may be involved in cytoskeletal and angiogenesis processes that are regulated by microtubule dynamics. TZT-1027 produces a unique genomic response profile distinct from that of *Vinca* alkaloids and taxanes, suggesting that this agent has a different mechanism of action. The selected genes may act as pharmacodynamic biomarkers allowing the unique mode of action of TZT-1027 to be discriminated from those of other antimicrotubule agents.
The Pharmacogenomics Journal advance online publication, 21 March 2006; doi:10.1038/sj.tpj.6500386

Keywords: TZT-1027; dolastatin 10; cDNA microarray; taxanes; *Vinca* alkaloids; antimicrotubule agent

Introduction

Dolastatin 10 (D10) is small peptide inhibiting microtubule assembly and tubulin polymerization that was isolated in 1987 from an Indian Ocean mollusc, the sea hare (*Dolabella auricularia*).[1] Although D10 displayed significant antitumor activity in preclinical models and demonstrated good tolerability in clinical settings, recent phase II clinical trials suggested that D10, as a single agent, lacked significant activity.[2–5] TZT-1027 is a synthesized derivative of D10 with superior preclinical activity.[6] TZT-1027 showed notable antitumor activity against a broad range of human malignancies *in vivo*, including those resistant to conventional chemotherapeutic agents.[7] Superior antivascular activity resulting in the collapse

of the tumor vasculature was demonstrated, compared with the activities of taxanes and *Vinca* alkaloids.[8–10] The first clinical phase I study of TZT-1027 was initiated in 1994, and another four studies have since been completed; a phase II study is currently ongoing.[11–13] The major toxicity was hematological, in the form of neutropenia and leukopenia. Reversible peripheral neurotoxic syndrome, alopecia, fatigue and anorexia were the principal nonhematological toxicities.

TZT-1027 is a mitotic spindle poison that interacts with tubulin at the *Vinca* alkaloids binding site,[14] but the spectra of antitumor activity of TZT-1027 and the *Vinca* alkaloids are different *in vivo*.[7,10,15] TZT-1027 also showed potent antitumor activity against a vincristine-resistant cell line.[7] A recent investigation of the mode of action reported that TZT-1027-induced apoptosis and cell arrest in the G_2/M phase that was independent of caspase-3 or bcl-2.[16] According to *in vitro* studies performed with tumor tissue obtained from patients with lung and renal cell cancers, the activity of TZT-1027 is influenced less by the p53 mutation status than by DNA-damaging agents.[17] Despite these investigations, the mode of action and therapeutic class of TZT-1027 as an antimicrotubule agent remains unclear. To characterize the mode of action of this compound, microarray-based transcriptional profiles have been performed.[18,19]

Cell-based high-throughput screening technologies provide information about cellular pathways that control drug sensitivity.[20,21] Drug-to-drug comparative approaches using microarray analyses are useful for identifying drug targets; the cellular effects caused by a novel drug of incompletely characterized specificity can be matched to 'reference profiles' of the cellular effects elicited by the specific inhibition of candidate analog-sensitive drugs.[22,23] Thus, it has been proposed that phenotypic information generated by drug-induced alterations in gene expression can be matched to discrete interactions between the compound and the relevant protein targets. Using the drug-to-drug comparative approach of the microarray analysis, we obtained reference profiles of genomic expression data from cellular responses in a lung cancer cell line to antimicrotubule drugs, including five conventional agents and the mother compound D10. In the present study, we aimed to characterize TZT-1027 using these reference profiles.

Results

Growth inhibition

The growth inhibitory effect of TZT-1027 and the other six antimicrotubule agents was determined using an MTT assay. The PC-14 cell line was exposed to each drug for 72 h. The 50% growth inhibitory concentrations (IC_{50} values) were as follows: TZT-1027, 0.02 nM; D10, 0.1 nM; VDS, 4 nM; VBL, 2 nM; VCR, 7 nM; TXL, 3 nM and TXT, 3 nM. Based on these results, TZT-1027 was over a hundred times more cytotoxic than the other taxanes and *Vinca* alkaloids.

Microarray data mining

The expression intensity of the array was normalized using a global normalization method. The change in gene expression was calculated as the intensity ratio between treated and untreated samples. The complete cDNA microarray data can be found in the Supplementary Tables. This supporting information contains the raw data, normalized data and a summary of the selected genes.

Common genes regulated by all antimicrotubule agents

Of the 588 genes that were surveyed in the microarray analysis, 118 genes were upregulated by all seven antimicrotubules

Table 1 Gene ontology analysis of biological process of antimicrotubule agents

Upregulated		*Downregulated*	
Gene category	P	*Gene category*	P
G2/M transition of mitotic cell cycle	<0.0001	Cell–cell signaling	<0.0001
Cytokinesis	<0.0001	Morphogenesis	<0.0001
Regulation of cell cycle	0.0002	Organogenesis	0.0001
Obsolete biological process	0.0003	Development	0.0001
G1/S transition of mitotic cell cycle	0.0004	Cell communication	0.0001
Mitotic cell cycle	0.0008	Positive regulation of cell proliferation	0.0042
Apoptosis	0.0009	Growth	0.0074
Cell cycle	0.0010	Immune response	0.0098
Programmed cell death	0.0012	Defense response	0.0098
Cell death	0.0012		
Death	0.0012		
Regulation of CDK activity	0.0012		
Positive regulation of programmed cell death	0.0077		
Positive regulation of apoptosis	0.0077		
Induction of apoptosis	0.0077		
Regulation of programmed cell death	0.0077		
Induction of programmed cell death	0.0077		

agents. A functional analysis of these genes was performed using EASE, and the results are listed in Table 1. The results showed that genes associated with cell-cycle regulation, mitosis or apoptosis were significantly upregulated by the antimicrotubules agents. Among the downregulated genes, 141 genes that were associated with cell communication and morphogenesis were selected. These results suggested that transcription regulation by antimicrotubule agents results in the biological inhibition of microtubule dynamics.

Drug characterization using molecular reference profiles

Focusing on the 'reference profiles' of the drug-induced genomic response, we compared the profiles of TZT-1027 with those of five conventional antimicrotubule agents and the mother compound, D10.

A principle component representation of the whole gene set in three-dimensional space clearly showed the relationship between TZT-1027 and the other six reference profiles (Figure 1). All the drugs were separated according to each drug class in this profile. In comparison with these reference profiles, TZT-1027's profile was similar to that of D10 but different from those of the taxanes and *Vinca* alkaloids.

To investigate the differences in genomic response between the drug classes, we selected discriminatory genes that were regulated differently between the drug classes, compared with the complete gene set. Table 2 shows the genes whose expression profiles differed after exposure to dolastatins (TZT-1027 and D10) and the other antimicrotubule agents. The most discriminatory gene in this gene set was the drug-resistant gene, *GSTO1*. Using this gene set, the classes of antimicrotubule agents could be clearly separated (Figure 2a). Discriminatory gene sets for the taxanes and *Vinca* alkaloids were obtained in a similar manner (Tables 3 and 4). The profiles of the discriminatory gene sets for the taxanes and *Vinca* alkaloids are shown in Figure 2b and c.

To further characterize TZT-1027, the genes that were regulated differently after exposure to TZT-1027 and D10 were investigated. Six genes that were regulated differently by a factor of more than one in a log ratio after exposure to each agent were selected (Table 5). Four cytoskeletal genes were included in this group. A three-dimensional representation using these six genes demonstrated that the profiles

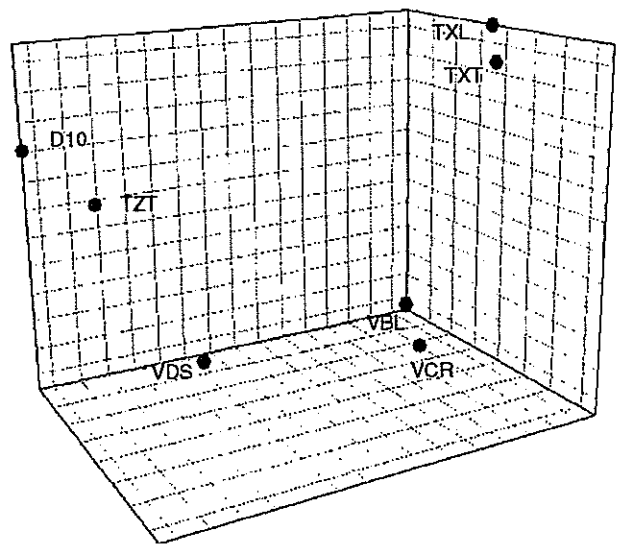

Figure 1 Three-dimensional representation of antimicrotubule agents according to a principle component analysis of the gene expression data for 588 genes. In this analysis, samples with similar expression profiles lie closer to each other than those with dissimilar profiles. The graph shows a robust class separation into three major categories: dolastatins, *Vinca* alkaloids and taxanes. TZT, TZT-1027; dolastatin 10, D10; VDS, vindesine; VCR, vincristine; VBL, vinblastine; TXL, paclitaxel; TXT, docetaxel.

Table 2 Discriminatory genes of dolastatins (D 10 and TZT-1027)

GB	*Symbol*	*Description*	*Log ratio*			
			D10	*TZT*	*VA*	*TX*
Upregulated genes						
U90313	GSTO1	Glutathione-*S*-transferase homolog	0.905	0.189	−0.818	−0.706
Z30183	TIMP3	Tissue inhibitor of metalloproteinase 3	0.703	0.481	−0.343	−0.859
U46461	DVL	Disheveled, dsh homolog 1	0.206	0.396	−0.542	−0.444
J00124	KRT1	50 kDa type I epidermal keratin	0.190	0.278	−0.643	−0.219
M57765	IL11	Interleukin 11	0.124	0.454	−0.342	−0.493
M74088	APC	Adenomatosis polyposis coli	0.040	0.069	−0.224	−0.582
Downregulated genes						
U02570	RhoGAP1	Rho-related small GTPase protein activator	−0.048	−0.076	0.433	0.248
J04177	COL11A1	Collagen, type XI, alpha 1	−0.048	−0.290	0.388	0.074
X72925	DSC1	Desmocollin-1	−0.117	−0.051	0.346	0.388
U35835	DNA-PK	DNA-dependent protein kinase	−0.215	−0.241	0.596	0.648
M65290	IL12B	Interleukin 12 beta	−0.322	−0.134	0.351	1.070

Abbreviations: GB, genebank accession number; D10, dolastatin 10; TZT, TZT-1027; VA, average of *Vinca* alkaloids including vincristine, vindesine, vinblastine; TX, average of taxanes including paclitaxel and docetaxel.

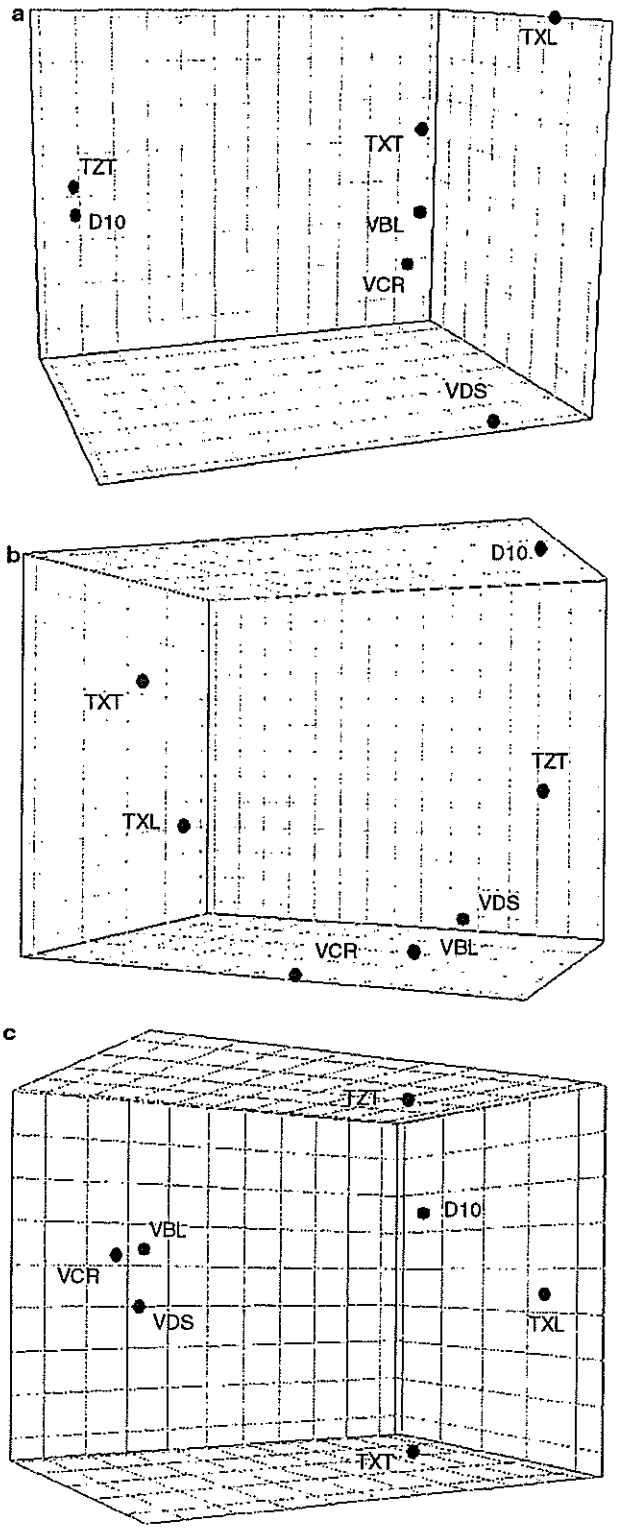

of the taxanes and *Vinca* alkaloids differed from those of TZT-1027 and D10 (Figure 3).

Validation of discriminatory genes by RT-PCR

The identified discriminatory genes GSTO1 and TIMP3 were validated using real-time RT-PCR (Figure 4). To investigate whether the genomic responses of these genes depended on the cytotoxicity levels, the RT-PCR experiment was performed at different cytotoxicity levels (IC_{90} and IC_{10}) of TZT-1027. The results are summarized in Figure 5. These findings suggested that the selected genomic responses might not depend on the cytotoxicity levels, whereas the genomic response of GSTO1 demonstrated a dose dependency.

Discussion

In the present study, we characterized the novel antimicrotubule agent TZT-1027 using a microarray analysis. Dolastatins belong to a class of microtubule-destabilizing agents, but this classification is not sufficient for clinical use. Despite similarities in their mechanism of action and structure, antimicrotubule agents differ in their antitumor and toxicologic profiles.[24] It now seems that the most important action of antimicrotubule agents is not the regulation of microtubule-polymer mass (polymerization and depolymerization), but the suppression of spindle-microtubule dynamics.[25] Furthermore, many of the drugs act not only on microtubules, but also on soluble tubulin, and the location of the specific binding site in tubulin and microtubules greatly affects the response of the microtubule system to the drug.[25] Therefore, to characterize the novel antimicrotubule agent TZT-1027, we analyzed drug-induced changes in gene expression using the microarray technique and compared the molecular profiles with those induced by the mother compound, D10, and other well-known antimicrotubule agents, such as *Vinca* alkaloids and taxanes.

For the profiles, we evaluated the IC_{50} value of each drug using a growth inhibitory assay. We aimed to categorize the drugs based on their mechanisms of action; therefore, the changes in gene expression were, of necessity, induced at the same cytotoxicity level. The resulting expression profiles were obtained using a microarray containing ~600 key genes applicable to antimicrotubule drug research, including genes involved with microtubule dynamics, cell-cycle regulation, angiogenesis and the extracellular matrix as well as cell adhesion receptors, oncogenes and tumor-suppressor genes. We focused on changes in gene expression because gene regulation should be correlated with the protein status modulated by the drugs.

Figure 2 Spatial class separation of antimicrotubule agents using specific discriminatory genes. The axes represent the first three linear discriminants of the expression levels of (a) 11 dolastatin-discriminatory genes from Table 2, (b) 9 taxane-discriminatory genes from Table 3 and (c) 5 *Vinca* alkaloid-discriminatory genes from Table 4. TZT, TZT-1027; dolastatin 10, D10; VDS, vindesine; VCR, vincristine; VBL, vinblastine; TXL, paclitaxel; TXT, docetaxel.

Table 3 Discriminatory genes of taxanes (paclitaxel, docetaxel)

GB	*Symbol*	*Description*	*Log ratio*			
			TX	*VA*	*D10*	*TZT*
Upregulated genes						
X02492	G1P3	Interferon-induced protein 6–16 precursor	1.122	−0.397	−1.150	−0.902
Y10256	NIK	Serine/threonine protein kinase	0.637	−0.951	−0.595	−0.287
U72661	NINJ1	Ninjurin 1	0.481	−0.154	−1.015	−0.448
M65199	ET2	Endothelin 2	0.444	−0.488	−2.185	−1.507
X54936	PlGF	Placenta growth factor	0.345	−0.235	−0.677	−0.602
X01992	IFN-gamma	Interferon, gamma	0.251	−0.929	−1.005	−1.583
Downregulated genes						
AF010309	PIG3	Tumor protein p53 inducible protein 3	−0.036	0.366	0.957	0.652
M76125	UFO	Tyrosine-protein kinase receptor UFO precursor	−0.132	0.201	0.020	0.329
U39657	MKK6	Mitogen-activated protein kinase 6	−0.204	0.554	0.740	0.368

Abbreviations: GB, genebank accession number; TX, average of taxanes including paclitaxel and docetaxel; VA, average of *Vinca* alkaloids including vincristine, vindesine, vinblastine; D10, dolastatin 10; TZT, TZT-1027.

Table 4 Discriminatory genes of *Vinca* alkaloids (vindesine, vincristine, vinblastine)

GB	*Symbol*	*Description*	*Log ratio*			
			VA	*TX*	*D10*	*TZT*
Upregulated genes						
X14787	TSP1	Thrombospondin 1	0.319	−0.230	−0.106	−0.019
X07820	MMP10	Matrix metalloproteinase 10	0.273	−0.272	−0.297	−0.417
Downregulated genes						
D78367	KRT12	Keratin 12	−0.124	0.262	0.250	0.598
X03212	KRT7	Keratin 7	−0.168	0.412	0.004	0.290
X56134	VIM	Vimentin	−1.072	0.583	0.927	1.344

Abbreviations: GB, genebank accession number; VA, average of *Vinca* alkaloids including vincristine, vindesine, vinblastine; TX, average of taxanes including paclitaxel and docetaxel; D10, dolastatin 10; TZT, TZT-1027.

Table 5 Discriminatory genes between TZT-1027 and dolastatin 10

GB	*Symbol*	*Description*	*Log ratio*						
			TZT	*D10*	*VDS*	*VBL*	*VCR*	*TXL*	*TXT*
U59167	DESM	Desmin	1.74	−0.49	−0.28	0.06	−0.71	0.44	0.43
U34819	MAPK10	Mitogen-activated protein kinase 10	0.83	−0.69	−0.52	0.98	0.57	1.33	0.93
X14420	COL3A1	Collagen, type III, alpha 1	0.52	−0.92	0.56	−0.79	−0.38	−0.67	−0.66
X05610	COL4A2	Collagen, type IV, alpha 2	0.71	−0.53	0.82	0.32	0.10	−0.06	0.33
X16468	COL2A1	Collagen, type II, alpha 1	1.08	−0.01	0.99	−0.08	0.56	0.36	−0.07
U33635	PTK7	Tyrosine-protein kinase-like 7	0.62	−0.45	0.04	0.56	0.68	0.15	0.05

Abbreviations: GB, genebank accession number; TZT, TZT-1027; D10, dolastatin 10; VDS, vindesine; VBL, vinblastine; VCR, vincristine; TXL, paclitaxel; TXT, docetaxel.

Of the 588 genes that were surveyed, about half of all the genes were regulated similarly by the seven drugs. The probability of these similar expression profiles occurring by chance is almost zero ($P<1\times10^{-100}$). Furthermore, the functions of the clustered genes were associated with microtubule dynamics. The 118 genes that were upregulated were significantly associated with cell-cycle regulation, mitosis or apoptosis, whereas the 141 genes that were

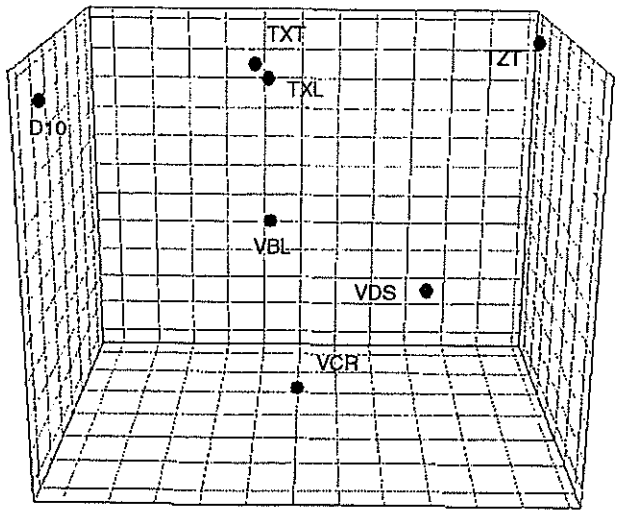

Figure 3 Spatial class separation of antimicrotubule agents using six genes from Table 5 that discriminated between TZT-1027 and dolastatin 10. TZT and D10 were distant from all the other antimicrotubule agents. TZT, TZT-1027; dolastatin 10, D10; VDS, vindesine; VCR, vincristine; VBL, vinblastine; TXL, paclitaxel; TXT, docetaxel.

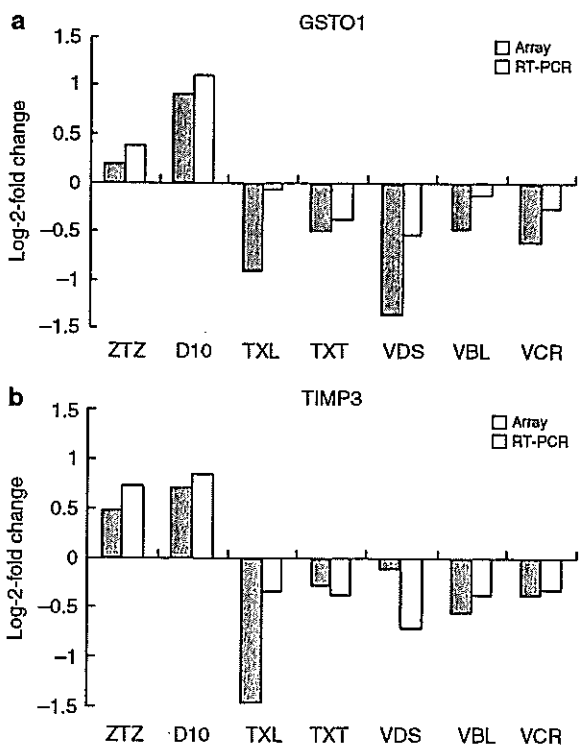

Figure 4 Gene expression of GSTO1 and TIMP3 in PC-14 cells treated with antimicrotubule agents. Validation of mRNA expression levels in PC-14 cells after 6 h of treatment with TZT-1027 (TZT), dolastatin 10 (D10), paclitaxel (TXL), docetaxel (TXT), vindesine (VDS), vinblastine (VBL) or vincristine (VCR). Relative mRNA amounts were normalized with respect to expression levels in untreated PC-14 cells (Log-2-fold change = 0).

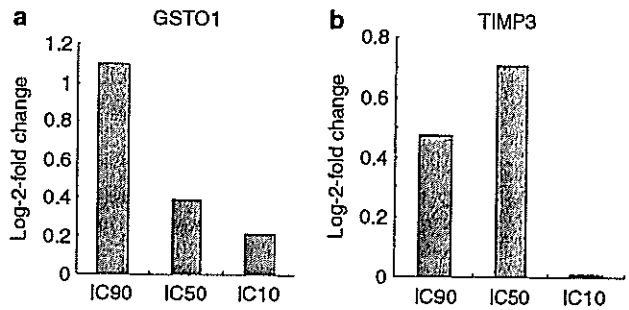

Figure 5 (a) Gene expression of GSTO1 in PC-14 cells treated with TZT-1027 at IC_{90}, IC_{50} or IC_{10}. (b) Gene expression of TIMP3 in PC-14 cells treated with TZT-1027 at IC_{90}, IC_{50} or IC_{10}. Validation of mRNA expression levels in PC-14 cells after 6 h of treatment with TZT-1027 (TZT) at IC_{90} (0.1 nM) or IC_{10} (0.005 nM).

downregulated were associated with cell communication and morphogenesis. Therefore, we concluded that the genomic response profiles represented the drug activities in PC-14 cells and investigated the discriminatory genes within each drug class to enable their further characterization.

By comparing the resulting gene profiles, each drug was categorized according to its drug class based on its effects on microtubule modulation (Figure 1). This finding suggested that genomic response was mostly affected by the drug-binding site on the microtubules. TXT shares the same tubulin-binding site as TXL, and this site is distinct from the *Vinca* alkaloids binding site.[25] Although TXL has a 1.9-fold higher affinity for the binding site and polymerizes tubulin at 2.1-fold lower concentrations than TXL,[26] TXL and TXT induced similar gene expression profiles, compared with those induced by the other antimicrotubule drugs. Among the three *Vinca* alkaloids (VBL, VDS and VCR), the expression profile of VDS differed from those of the other two (Figure 6). Natsume *et al.*[14] reported that all three *Vinca* alkaloids inhibited the polymerization of microtubules at a similar affinity. VBL and VCR are structurally very similar, whereas the structure of VDS differs from those of the other two.[27] This structural difference may be responsible for the different genomic responses. *Vinca* alkaloids and dolastatins are known to bind at so-called *Vinca*-binding domains in tubulin.[25] They share the same binding site and have similar affinities,[14,28] whereas additional binding sites have either high affinities (Kd: 1–2 μmol) or low affinities (Kd: 0.25–3 μmol).[24] Previous studies have also reported that dolastatins can also bind at different sites from those used by *Vinca* alkaloids[14,29] These additional binding sites might be responsible for the differences in genomic response induced by the dolastatins and *Vinca* alkaloids.

Interestingly, of the 31 discriminatory genes that were selected, six of them were intermediate filament (IF) genes like desmin, vimentin, desmocollin and keratin (Tables 2, 4, 5). In addition, four collagen genes and one Rho-regulator gene were also selected. These genes are all associated with cytoskeletal regulation by the Rho signaling pathway via

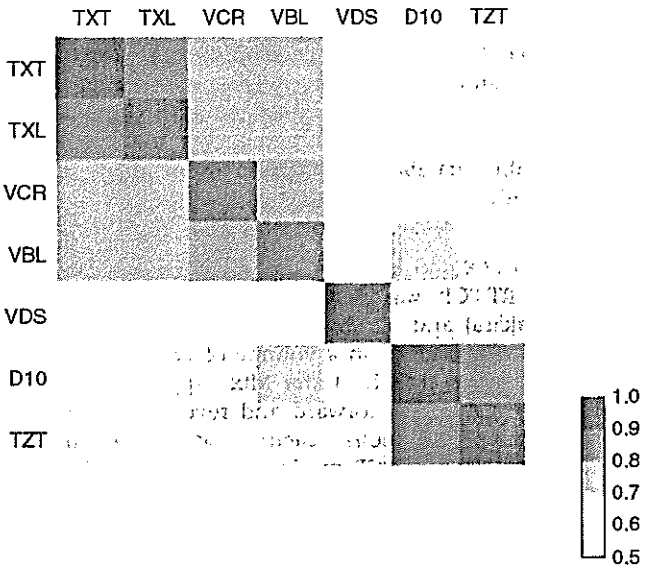

Figure 6 Heat map of correlations between drug profiles. Gene expression profiles containing data for 588 genes were compared after exposure to each drug to derive a matrix of Pearson correlation coefficients indicating the degree of overall similarity between any two drugs. A high-positive correlation is shown in red, and a low-positive correlation is shown in white. In this graph, TZT and D10 had the most similar expression profiles. TZT, TZT-1027; dolastatin 10, D10; VDS, vindesine; VCR, vincristine; VBL, vinblastine; TXL, paclitaxel; TXT, docetaxel.

microtubule dynamics.[30] Rho proteins also modulate the extracellular matrix either by regulating the levels of MMPs (matrix metalloproteinase) or their antagonists, TIMPs (tissue inhibitor of metalloproteinase).[31] These results suggested that the difference in the tubulin-drug binding site might regulate the difference in the signal transduction.

Of the genes that discriminated between dolastatins and the other drug class, the most significant genes were GSTO1 and TIMP3. GSTO1 (glutathione transferase omega 1) is a member of the glutathione *S*-transferase (GST) family of phase II enzymes that catalyze glutathione-dependent detoxification.[32] The role of GST has been evaluated in drug resistance. Schisselbauer *et al.* [33]reported that an elevated GST level in tumors was detected after the development of clinical drug resistance. Ban *et al.*[34] reported that adriamycin, cisplatin and etoposide increased tumor sensitivity by inhibiting GST expression in a colon cancer cell line, but TXL and VCR did not alter sensitivity. TIMP3 is a protein that binds to the extracellular matrix[35] and belongs to a family of endogenous MMP inhibitors. Members of the MMP family play important roles in angiogenesis.[36] Therefore, TIMP3 is regarded as a potent inhibitor of angiogenesis and tumor growth.[37] Qi *et al.*[38] reported that TIMP3 blocks the binding of VEGF (vascular endothelial growth factor) to the VEGF receptor-2, inhibiting downstream signaling and angiogenesis. TZT-1027 showed antitumor activity *in vivo* against a hypervascular advanced-stage tumor from a VEGF-transfectant lung cancer cell line, whereas VCR and TXT did not.[10] The upregulation of TIMP3 by TZT-1027 is one possible mechanism for the superior antivascular activity of this drug, compared to that of taxanes and *Vinca* alkaloids.

To analyze whether similar genomic responses occurred in lung cancer cell lines other than PC-14, RT-PCR for GSTO1 and TIMP3 was performed in another lung cancer cell line, SBC-3, treated with TZT-1027 at IC_{50}. GSTO1 and TIMP3 were downregulated in SBC-3 cells treated with dolastatins and upregulated in the cells treated with the other antimicrotubule agents, opposite to the profile seen for PC-14 cells (data not shown). This result suggested that these genes may have different genomic responses in other lung cancer cells.

This was a 'proof-of-principle study'. We demonstrated the various cellular responses to antimicrotubule agents at a gene expression level, even though the agents targeted the same molecules. We believe that this approach to characterizing drugs *in vitro* may be useful in clinical settings in that surrogate tissue, like peripheral blood mononuclear cells, can be used. The present findings obtained using our microarray analysis could greatly help us to understand the mode of action of TZT-1027 and other antimicrotubule agents. This capacity to identify therapeutic efficacy on the basis of gene expression signatures *in vitro* may be useful for drug discovery and drug target validation.

Materials and methods

Cell lines and cultures

A human non-small-cell-lung cancer cell line, PC-14, was provided by Professor Y Hayata, Tokyo Medical College. PC-14 was grown in RPMI-1640 medium (Nikken BioMedical Laboratory, Kyoto, Japan) supplemented with 10% fetal bovine serum, penicillin G and 100 μg/ml streptomycin solution and was maintained in a humidified 5% CO_2 atmosphere at 37°C.

Drugs and culture

TZT-1027 and D10 were provided by Teikoku Hormone Mfg. Co. Ltd (Kawasaki, Japan) and were dissolved in and diluted with 0.05 M lactate buffer (pH 4.5). Vindesine (VDS), vincristine (VCR), vinblastine (VBL), docetaxel (TXT) and paclitaxel (TXL) were obtained from Shionogi Co. (Osaka, Japan), Shionogi Pharmaceutical Co. (Osaka, Japan), Kyorin Pharmaceutical Co. Ltd (Tokyo, Japan), Chugai-Seiyaku Co, Ltd (Tokyo, Japan) and Bristol-Myers Japan (Tokyo, Japan), respectively. RPMI 1640 medium (Gibe-BRL) and fetal bovine serum were purchased from Nisus (Tokyo, Japan).

MTT assay

The inhibitory effect of the drugs on the PC-14 cell line was determined using a colorimetric assay (MTT assay) according to the method of Mosmann.[39] Briefly, 10^3 cells were harvested in 96-well microtiter plates (Becton Dickinson & Co.) in a volume of 180 μl and incubated for 24 h at 37°C in humidified air containing 5% CO_2. Each drug was added to

individual wells in a volume of 20 μl, and the cells were incubated for 72 h at 37°C in humidified air containing 5% CO_2. MTT reagents (MTT, Sigma) were then added to each well in a volume of 20 μl, and the cells were incubated for 4 h at 37°C in humidified air containing 5% CO_2. Finally, the growth inhibitory effect of each drug was assessed spectrophotometrically.

Drug treatment, RNA isolation and microarray hybridization

To obtain reference profiles representing the drug-induced genomic response, the PC-14 cells were grown on plastic culture dishes until they reached 80% confluency; they were then treated with TZT-1027, D10, VDS, VCR, VBL, TXL and TXT for 6 h at the IC_{50} concentration of each drug determined by MTT assay for 72 h. Cell pellets of the eight samples, including an untreated control, were collected by centrifugation, and the total RNA from each sample was isolated using a single-step guanidium thiocyanate procedure (ISOGEN; Nippon gene).[40] Single-channel labeling ^{32}P nylon membrane-based cDNA microarrays containing 588 genes were used (Atlas® Human Cancer cDNA Expression Array; BD Biosciences Clontech, Palo Alto, CA, USA). Protocols on array printing, labeling and hybridization are available at the BD Biosciences Clontech web site (http://www.bdbiosciences.com/clontech/atlas/index.shtml) The hybridization intensities on X-ray films (Gel Bond®, FMC Bio Products Rockland, ME, USA) were scanned and quantified using a BAS-2000II scanner and Array Gauge software (Fuji Film, Tokyo).

Microarray data analysis

The intensity values of each gene were log-2-transformed and median-normalized using Excel software. The changes in gene expression induced by drug exposure were calculated for each spot by dividing the intensity of the drug exposure samples by that of the untreated samples. The multidimensional scaling analysis, based on a principle component analysis, was performed using SIMCA-P software v10.5 (Umetrics, Sweden). Three-dimensional rendering of the gene profiles was graphed in a manner such that samples with similar expression profiles would lie closer to each other than those with dissimilar profiles. The heat map, which showed the correlation coefficient between each drug reference profile, was performed by *R* (http://cran.r-project.org/).

Functional analysis of identified genes

To analyze the functions of the clustered genes, a gene ontology analysis was performed using the EASE bioinformatics software package (http://apps1.niaid. nih.gov/david/upload.asp).[41,42] This software package was used to rank functional clusters by statistical over-representation of individual genes in specific categories relative to all genes in the same category on the array. The functional clusters used by EASE were derived from the classification systems of Gene Ontology (GO). The *P*-value to rank categories of genes by over-representation was calculated using Jackknife-Fisher exact probabilities. The threshold for selecting categories was a *P*-value of less than 0.01 and a minimum gene count of more than two. *P*-values in gene ontology are not equal to biological significance but are helpful in focusing on the processes most likely to be associated with the biological phenomena associated with aging. We also conducted further online database searches to refine many specific GO annotations.

Real-time RT-PCR

Real-time RT-PCR was performed using a Smart Cycler system (Takara) and a SYBR Green PCR kit. The reaction solution was assembled in a volume of 25 μl comprised of TaqMan™ Universal PCR Master Mix (Applied Biosystems, Foster City, CA, USA), forward and reverse primers (final concentration, 0.2 μmol/l each) and cDNA mixture ($\approx$2.5 ng) to produce PCR products specific for *GSTP1* and *TIMP3*. The primers and probes were purchased from Sigma-GenoSys (Tokyo, Japan). The conditions for real-time RT-PCR were preheating at 95°C for 10 min, followed by 40 cycles of shuttle heating at 95°C for 15 s and at 60°C for 20 s. A threshold was set in the linear part of the amplification curve, and the number of cycles needed to reach it was calculated for every gene. Relative mRNA levels were determined using the included standard curves for each individual gene and further normalized to the GAPDH mRNA level. Melting curves were used to establish the purity of the amplified band. The sequences of the primers used for RT-PCR were as follows: GSTO1 forward, 5′-AGG TTC TGC CCG TTT GCT GAG AGG and reverse, 5′-CAA GCT TTC TCA TAG GGG TCA TCC G; TIMP3 forward, 5′-TGC TGA CAG GTC GCG TCT ATG ATG G and reverse, 5′-GCG TAG TGT TTG GAC TGG TAG CCA G; GAPDH forward, 5′-TGA AGG TCG GAG TCA ACG GAT TTG GT and reverse, 5′-CAT GTG GGC CAT GAG GTC CAC CAC.

Acknowledgments

This study was supported in part by a Grant-in-Aid for Cancer Research and the 3rd Term Comprehensive 10-Year Strategy for Cancer Control from the Ministry of Health, Labour and Welfare, Tokyo, Japan. K Nishio and T Shimoyama designed the study. T Shimoyama and K Nishio prepared the manuscript. Y Koh and T Natsume undertook the study. T Shimoyama and T Hamano performed the statistical analysis. T Shimoyama is the recipient of a Research Resident Fellowship from the Foundation of Promotion of Cancer Research in Japan.

Duality of Interest

None declared.

References

1 Pettit G, Kamano Y, Herald C, Tuinman A, Boettner F, Kizu H *et al.* The isolation and structure of a remarkable marine animal antineoplastic constituent: dolastatin 10. *J Am Chem Soc* 1987; 109: 6883–6885.
2 Saad ED, Kraut EH, Hoff PM, Moore Jr DF, Jones D, Pazdur R *et al.* Phase II study of dolastatin-10 as first-line treatment for advanced colorectal cancer. *Am J Clin Oncol* 2002; 25: 451–453.

3 Vaishampayan U, Glode M, Du W, Kraft A, Hudes G, Wright J *et al.* Phase II study of dolastatin-10 in patients with hormone-refractory metastatic prostate adenocarcinoma. *Clin Cancer Res* 2000; 6: 4205–4208.
4 Krug LM, Miller VA, Kalemkerian GP, Kraut MJ, Ng KK, Heelan RT *et al.* Phase II study of dolastatin-10 in patients with advanced non-small-cell lung cancer. *Ann Oncol* 2000; 11: 227–228.
5 Margolin K, Longmate J, Synold TW, Gandara DR, Weber J, Gonzalez R *et al.* Dolastatin-10 in metastatic melanoma: a phase II and pharmokinetic trial of the California Cancer Consortium. *Invest New Drugs* 2001; 19: 335–340.
6 Miyazaki K, Kobayashi M, Natsume T, Gondo M, Mikami T, Sakakibara K *et al.* Synthesis and antitumor activity of novel dolastatin 10 analogs. *Chem Pharm Bull (Tokyo)* 1995; 43: 1706–1718.
7 Kobayashi M, Natsume T, Tamaoki S, Watanabe J, Asano H, Mikami T *et al.* Antitumor activity of TZT-1027, a novel dolastatin 10 derivative. *Jpn J Cancer Res* 1997; 88: 316–327.
8 Chaplin DJ, Pettit GR, Parkins CS, Hill SA. Antivascular approaches to solid tumour therapy: evaluation of tubulin binding agents. *Br J Cancer Suppl* 1996; 27: S86–S88.
9 Otani M, Natsume T, Watanabe JI, Kobayashi M, Murakoshi M, Mikami T *et al.* TZT-1027, an antimicrotubule agent, attacks tumor vasculature and induces tumor cell death. *Jpn J Cancer Res* 2000; 91: 837–844.
10 Natsume T, Watanabe J, Koh Y, Fujio N, Ohe Y, Horiuchi T *et al.* Antitumor activity of TZT-1027 (Soblidotin) against vascular endothelial growth factor-secreting human lung cancer *in vivo*. *Cancer Sci* 2003; 94: 826–833.
11 Niitani H, Hasegawa K. Phase I studies of TZT-1027, a novel inhibitor of tubulin polymerization. *Ann Oncol* 1998; 9(Suppl 2): 360.
12 de Jonge MJ, van der Gaast A, Planting AS, van Doorn L, Lems A, Boot I *et al.* Phase I and pharmacokinetic study of the dolastatin 10 analogue TZT-1027, given on days 1 and 8 of a 3-week cycle in patients with advanced solid tumors. *Clin Cancer Res* 2005; 11: 3806–3813.
13 Schoffski P, Thate B, Beutel G, Bolte O, Otto D, Hofmann M *et al.* Phase I and pharmacokinetic study of TZT-1027, a novel synthetic dolastatin 10 derivative, administered as a 1-hour intravenous infusion every 3 weeks in patients with advanced refractory cancer. *Ann Oncol* 2004; 15: 671–679.
14 Natsume T, Watanabe J, Tamaoki S, Fujio N, Miyasaka K, Kobayashi M. Characterization of the interaction of TZT-1027, a potent antitumor agent, with tubulin. *Jpn J Cancer Res* 2000; 91: 737–747.
15 Fujita F, Koike M, Fujita M, Sakamoto Y, Tsukagoshi S. Antitumor effects of TZT-1027, a novel dolastatin 10 derivative, on human tumor xenografts in nude mice. *Gan To Kagaku Ryoho* 2000; 27: 451–458.
16 Watanabe J, Natsume T, Fujio N, Miyasaka K, Kobayashi M. Induction of apoptosis in human cancer cells by TZT-1027, an antimicrotubule agent. *Apoptosis* 2000; 5: 345–353.
17 Natsume T, Kobayashi M, Fujimoto S. Association of p53 gene mutations with sensitivity to TZT-1027 in patients with clinical lung and renal carcinoma. *Cancer* 2001; 92: 386–394.
18 Natsume T, Nakamura T, Koh Y, Kobayashi M, Saijo N, Nishio K. Gene expression profiling of exposure to TZT-1027, a novel microtubule-interfering agent, in non-small cell lung cancer PC-14 cells and astrocytes. *Invest New Drugs* 2001; 19: 293–302.
19 DeRisi JL, Iyer VR, Brown PO. Exploring the metabolic and genetic control of gene expression on a genomic scale. *Science* 1997; 278: 680–686.
20 Parsons AB, Brost RL, Ding H, Li Z, Zhang C, Sheikh B *et al.* Integration of chemical-genetic and genetic interaction data links bioactive compounds to cellular target pathways. *Nat Biotechnol* 2004; 22: 62–69.
21 Baetz K, McHardy L, Gable K, Tarling T, Reberioux D, Bryan J *et al.* Yeast genome-wide drug-induced haploinsufficiency screen to determine drug mode of action. *Proc Natl Acad Sci USA* 2004; 101: 4525–4530.
22 Kung C, Kenski DM, Dickerson SH, Howson RW, Kuyper LF, Madhani HD *et al.* Chemical genomic profiling to identify intracellular targets of a multiplex kinase inhibitor. *Proc Natl Acad Sci USA* 2005; 102: 3587–3592.
23 Gunther EC, Stone DJ, Gerwien RW, Bento P, Heyes MP. Prediction of clinical drug efficacy by classification of drug-induced genomic expression profiles *in vitro*. *Proc Natl Acad Sci USA* 2003; 100: 9608–9613.
24 DeVita VT, Hellman S, Rosenberg SA. *Cancer: Principles and Practice of Oncology*, 7th edn, Lippincott Williams & Wilkins (LWW): Philadelphia, 2004.
25 Jordan MA, Wilson L. Microtubules as a target for anticancer drugs. *Nat Rev Cancer* 2004; 4: 253–265.
26 Diaz JF, Andreu JM. Assembly of purified GDP-tubulin into microtubules induced by taxol and taxotere: reversibility, ligand stoichiometry, and competition. *Biochemistry* 1993; 32: 2747–2755.
27 Jordan A, Hadfield JA, Lawrence NJ, McGown AT. Tubulin as a target for anticancer drugs: agents which interact with the mitotic spindle. *Med Res Rev* 1998; 18: 259–296.
28 Gupta S, Bhattacharyya B. Antimicrotubular drugs binding to *Vinca*domain of tubulin. *Mol Cell Biochem* 2003; 253: 41–47.
29 Bai RL, Paull KD, Herald CL, Malspeis L, Pettit GR, Hamel E. Halichondrin B and homohalichondrin B, marine natural products binding in the *Vinca*domain of tubulin. Discovery of tubulin-based mechanism of action by analysis of differential cytotoxicity data. *J Biol Chem* 1991; 266: 15882–15889.
30 Etienne-Manneville S, Hall A. Rho GTPases in cell biology. *Nature* 2002; 420: 629–635.
31 Sahai E, Marshall CJ. RHO-GTPases and cancer. *Nat Rev Cancer* 2002; 2: 133–142.
32 Board PG, Coggan M, Chelvanayagam G, Easteal S, Jermiin LS, Schulte GK *et al.* Identification, characterization, and crystal structure of the Omega class glutathione transferases. *J Biol Chem* 2000; 275: 24798–24806.
33 Schisselbauer JC, Silber R, Papadopoulos E, Abrams K, LaCreta FP, Tew KD. Characterization of glutathione S-transferase expression in lymphocytes from chronic lymphocytic leukemia patients. *Cancer Res* 1990; 50: 3562–3568.
34 Ban N, Takahashi Y, Takayama T, Kura T, Katahira T, Sakamaki S *et al.* Transfection of glutathione S-transferase (GST)-pi antisense complementary DNA increases the sensitivity of a colon cancer cell line to adriamycin, cisplatin, melphalan, and etoposide. *Cancer Res* 1996; 56: 3577–3582.
35 Anand-Apte B, Bao L, Smith R, Iwata K, Olsen BR, Zetter B *et al.* A review of tissue inhibitor of metalloproteinases-3 (TIMP-3) and experimental analysis of its effect on primary tumor growth. *Biochem Cell Biol* 1996; 74: 853–862.
36 Hiraoka N, Allen E, Apel IJ, Gyetko MR, Weiss SJ. Matrix metalloproteinases regulate neovascularization by acting as pericellular fibrinolysins. *Cell* 1998; 95: 365–377.
37 Anand-Apte B, Pepper MS, Voest E, Montesano R, Olsen B, Murphy G *et al.* Inhibition of angiogenesis by tissue inhibitor of metalloproteinase-3. *Invest Ophthalmol Vis Sci* 1997; 38: 817–823.
38 Qi JH, Ebrahem Q, Moore N, Murphy G, Claesson-Welsh L, Bond M *et al.* A novel function for tissue inhibitor of metalloproteinases-3 (TIMP3): inhibition of angiogenesis by blockage of VEGF binding to VEGF receptor-2. *Nat Med* 2003; 9: 407–415.
39 Mosmann T. Rapid colorimetric assay for cellular growth and survival: application to proliferation and cytotoxicity assays. *J Immunol Methods* 1983; 65: 55–63.
40 Chomczynski P, Sacchi N. Single-step method of RNA isolation by acid guanidinium thiocyanate-phenol-chloroform extraction. *Anal Biochem* 1987; 162: 156–159.
41 Hosack DA, Dennis Jr G, Sherman BT, Lane HC, Lempicki RA. Identifying biological themes within lists of genes with EASE. *Genome Biol* 2003; 4: R70.
42 Dennis Jr G, Sherman BT, Hosack DA, Yang J, Gao W, Lane HC *et al.* DAVID: database for annotation, visualization, and integrated discovery. *Genome Biol* 2003; 4: P3.

Supplementary Information accompanies the paper on The Pharmacogenomics Journal website (http://www.nature.com/tpj).

Int. J. Cancer: 118, 483–489 (2006)
© 2005 Wiley-Liss, Inc.

ZD6474 inhibits tumor growth and intraperitoneal dissemination in a highly metastatic orthotopic gastric cancer model

Tokuzo Arao[1,2,4], Kazuyoshi Yanagihara[3], Misato Takigahira[3], Masayuki Takeda[1,2], Fumiaki Koizumi[1,2], Yasushi Shiratori[4] and Kazuto Nishio[1,2]*

[1]*Shien Lab, Medical Oncology, National Cancer Center Hospital, Tokyo, Japan*

[2]*Pharmacology Division, National Cancer Center Research Institute, Tokyo, Japan*

[3]*Central Animal Laboratory, National Cancer Center Research Institute, Tokyo, Japan*

[4]*Department of Gastroenterology and Hepatology, Okayama University Graduate School of Medicine and Dentistry, Okayama, Japan*

Angiogenesis inhibitors have been used to treat some cancers, but the therapeutic potential of these agents for gastric cancer has remained unclear. To investigate their therapeutic potential, we examined the effect of ZD6474, an agent that selectively targets vascular endothelial growth factor receptor-2 (VEGFR-2; KDR) tyrosine kinase and epidermal growth factor receptor (EGFR) tyrosine kinase, in a highly metastatic orthotopic model using an undifferentiated gastric cancer cell line, 58As1. ZD6474 (100 mg/kg/day, p.o., 2 weeks) significantly inhibited tumor growth ($p < 0.05$ *vs.* control) and reduced tumor dissemination into the peritoneal cavity ($p < 0.05$ *vs.* control). In addition, to identify putative tumor biomarkers that would reflect the effects of ZD6474 treatment in clinical settings, we examined the gene expression profiles of implanted gastric tumors treated with ZD6474 *in vivo*. Twenty-eight candidate genes were identified, including *IGFBP-3*, *ADM*, *ANGPTL4*, *PLOD2*, *DSIPI*, *NDRG1*, *ENO2*, *HIG2* and *BNIP3L*, which are known to be hypoxia-inducible genes. These genes and gene products may be useful biomarkers for monitoring the effects of ZD6474 treatment. ZD6474 also improved the survival of mice with implanted another undifferentiated gastric cancer cell line, 44As3. In conclusion, our results suggest that ZD6474 may have clinical activity against gastric cancer, particularly undifferentiated gastric cancer with peritoneal dissemination. We also identified putative biomarkers for monitoring the pharmacodynamic effects of ZD6474 by gene expression profiling.
© *2005 Wiley-Liss, Inc.*

Key words: ZD6474; gastric cancer; intraperitoneal dissemination; VEGF; oligonucleotide microarray

Various anti-cancer agents have been examined for efficacy against gastric cancer over the past two decades, but the median survival time of patients remains around 7 months,[1,2] and the prognosis of gastric cancer patients remains poor. Peritoneal dissemination is common in patients with unresectable gastrointestinal cancer, and many suffer from peritoneal carcinomatosis in the terminal stage. Because undifferentiated gastric cancer is particularly invasive and often accompanied by peritoneal dissemination,[3] a new treatment strategy is needed.

Vascular endothelial growth factor (VEGF) is a key mediator of tumor growth and is known to have multiple functions in angiogenesis, vascular permeability, and the regulation of endothelial cell proliferation and migration.[4–6] VEGF receptors (VEGFR) are activated by ligand stimulation with VEGF and commonly expressed in vascular endothelial cells. VEGFR-2 (KDR/Flk-1) is thought to be important for angiogenesis.[7] Because the VEGF-VEGFR system plays a key role in angiogenesis and tumor growth *in vivo*, the therapeutic potential of many agents targeting this system is being investigated.[8] A recent study has shown that a combination of monoclonal antibody against VEGF and chemotherapy produces a clinically meaningful survival benefit for patients with metastatic colorectal cancer,[5] and these results may lead to changes in the standard treatment for colorectal cancer.[9]

ZD6474 is a novel orally available VEGFR-2 (KDR) tyrosine kinase inhibitor that is also known to selectively target epidermal growth factor receptor (EGFR) tyrosine kinase, both of which are parts of key pathways in tumor growth.[10–13] We demonstrated previously the evidence suggesting that ZD6474 inhibits angiogenesis and tumor growth by targeting EGFR.[14,15]

In our present study, we tested ZD6474 for an inhibitory effect on tumor growth and intraperitoneal dissemination, and for improvement of survival in a newly established, highly metastatic orthotopic gastric tumor model *in vivo*. In addition, we also identified putative biomarkers to monitor the effects of ZD6474 treatment using gene expression profiling.

Material and methods

Reagents

ZD6474 and gefitinib (Iressa®) were provided by AstraZeneca (Cheshire, UK).

Cell cultures

The newly established highly metastatic human signet-ring cell gastric cancer cell lines 58As1 and 44As3 produce large volumes of ascitic fluid and spontaneously metastasize to the peritoneal cavity after orthotopic (gastric wall) implantation.[16,17] 58As1 and 44As3 and human non-small cell lung cancer cell line PC-9 were maintained in RPMI-1640 medium (Sigma, St. Louis, MO) supplemented with 10% heat-inactivated FBS (Gibco BRL, Grand Island, NY). The PC-9 cells were a gift of Tokyo Medical University. Human embryonic kidney cell line 293 (HEK293) was obtained from the American Type Culture Collection (Manassas, VA) and cultured in DMEM supplemented with 10% FBS. Human umbilical vein endothelial cells (HUVEC) were maintained in EBM-2 medium (Clonetics, Walkersville, MD) supplemented with EGM-2 kit (Clonetics), according to the manufacturer's instructions.

In vitro *growth-inhibition assay*

The cell-growth inhibitory effects of ZD6474 and gefitinib were assessed by the thiazole blue tetrazolium bromide (MTT) assay (Sigma). Briefly, 180 μl/well of cell suspension was seeded on to Sumilon® 96-well microculture plates (Sumitomo Bakelite, Akita, Japan) and incubated in 10% FBS-containing medium for 24 hr. The cells were then treated with ZD6474 at various concentrations (4 nM–80 μM) and cultured at 37°C in a humidified atmosphere for 72 hr. After the culture period, 20 μl volume of MTT reagent was added, and the plates were further incubated for 4 hr. After centrifuging the plates, the culture medium was discarded and the wells were filled with dimethyl-sulfoxide. The optical density of the cultures was measured at 562 nm with Delta-soft software on a

Grant sponsor: Ministry of Education, Culture, Sports, Science and Technology of Japan; Grant number: 12217165.

*Correspondence to: Shien Lab, Medical Oncology, National Cancer Center Hospital, Tsukiji 5-1-1, Chuo-ku, Tokyo 104-0045, Japan. Fax: +81-3-3547-5185. E-mail: knishio@gan2.res.ncc.go.jp

Received 14 March 2005; Accepted after revision 18 May 2005
DOI 10.1002/ijc.21340
Published online 28 July 2005 in Wiley InterScience (www.interscience.wiley.com)

Macintosh computer interfaced to a Bio-Tek Microplate Reader EL-340 (BioMetallics, Princeton, NJ). The experiment was conducted in triplicate.

Immunoblotting

EGFR, phospho-EGFR (specific for Tyr 1068), and anti-rabbit horseradish peroxidase (HRP)-conjugated antibody were purchased from Cell Signalling (Beverly, MA). Cell pellets were lysed in RIPA buffer (Tris-HCl, 50 mM; pH 7.4; NP-40, 1%; Na-deoxycholate, 0.25%; NaCl, 150 mM; EDTA, 1 mM; phenylmethyl-sulfonyl fluoride, 1 mM; aprotinin, leupeptin, pepstatin, 1 mg/ml each; Na_3VO_4, 1 mM; NaF, 1 mM). Cell extracts were electrophoresed on 7.5% (w/v) polyacrylamide gels and transferred to a polyvinylidene di-fluoride membrane (Nihon Millipore, Tokyo, Japan). The membrane was incubated in Tris-buffered saline containing 0.5% Tween 20 with 3% BSA and then reacted with the primary antibodies and the HRP-conjugated secondary antibody for 90 min each. Visualization was achieved with an enhanced chemiluminescent detection reagent (Amersham Bioscience, Buckinghamshire, UK).

RT-PCR

A 5 μg of total RNA from each cultured cell line was converted to cDNA with a GeneAmp® RNA-PCR kit (Applied Biosystems, Foster City, CA). The primers used for the PCR were: human-specific beta-actin, forward: 5′-GGAAATCGTGCGTGACATT-3′ and reverse: 5′-CATCTGCTGGAAGGTGGACAG-3′; mouse-specific beta-actin, forward: 5′-GAAATCGTGCGTGACATCAAA-3′ and reverse: 5′-TCATGGTGCTAGGAGCCA-3′; VEGF-A, forward: 5′-GCCTTG-CCTTGCTGCTCTAC-3′ and reverse: 5′-CA-GGGATTTTCTTGTC-TTGC-3′; VEGF-C, forward: 5′-AAACAAGGAGCTGGATGAA-GAG-3′ and reverse: 5′-CAATATGAAGGGACACAACGAC-3′; VEGFR-1, forward: 5′-TAGCGTCACCAGCAGCGAAAGC-3′ and reverse: 5′-CCTTTCTTTTGGGTCTCTGTGC-3′; VEGFR-2, forward: 5′-CAGACGGAC-AGTGGTATGGTTC-3′ and reverse: 5′-ACCTGCTGGTGGAAAGAACAAC-3′; VEGFR-3, forward: 5′-AGCCATTCATCAACAAGCCT-3′ and reverse: 5′-GGCAACAG-CTGGATGTCATA-3′; IGFBP3, forward: 5′- AATGCTAGTGA-GTCGGAGGAAGAC-3′ and reverse: 5′- GGCGACACTGCTTTT-TCTTATAAA-3′; ADM, forward: 5′- CCTGGGTTCGCTCGCCTT-CCTA-3′ and reverse: 5′- GGCTGGAGCCCCGTGTG- CTTGT-3′.

PCR amplification was carried out for 35 cycles (95°C for 45 sec, 56–62°C for 45 sec, and 72°C for 60 sec) with a final extension step at 72°C for 7 min. The bands were visualized by ethidium bromide staining.

Sequencing

Exons 18–21 of the EGFR cDNA from the tumor cell lines were sequenced, and the cDNAs were amplified using the following primers: forward, 5′-TCCAAACTGCACCTACGGATGC-3′, and reverse, 5′-CATCAACTCCCAAACGGTCACC-3′. The PCR amplification consisted of 25 cycles (95°C for 45 sec, 55°C for 30 sec and 72°C for 60 sec). The sequences of the PCR products were determined using ABI prism 310 (Applied Biosystems). Amplification and sequencing were carried out in duplicate for each tumor cell line. The sequences were compared to the GenBank-archived human sequence of EGFR (accession number: NM_005228.3).

Orthotopic model in vivo

ZD6474 was dissolved in sterile water containing 1% TWEEN 80 (Sigma). Six-week old female BALB/c nude mice were purchased from CLEA Japan Inc. (Tokyo) and maintained under specific pathogen-free conditions. A total of 1×10^6 58As1 cells was inoculated into the gastric wall of each mouse after laparotomy. Three days after the inoculation, the mice were given ZD6474 50 mg/kg/day ($n = 6$) or 100 mg/kg/day ($n = 6$) or a vehicle control ($n = 6$) p.o. for 14 days. After euthanizing the mice on Day 19, tumor volume was measured and tumor samples and intraperitoneal lavage fluid were collected. The tumor samples were formalin fixed ($n = 3$) or stored in Isogen ($n = 3$) (Nippon Gene, Tokyo, Japan). The intraperitoneally disseminated cells were collected from 2 ml of PBS that had been used to wash the peritoneal cavity.

In the survival study, mice were inoculated with 1×10^6 58As1 or 44As3 cells into the gastric wall after laparotomy. Three days after inoculation, the mice were given ZD6474 50 mg/kg/day of ZD6474 p.o. ($n = 7$) or i.p. ($n = 7$) or the vehicle control p.o. ($n = 7$) for 14 days. The "visible ascites," which was evident a few days before death in this model, was used as a surrogate for survival time to consider for animal welfare. Mice were euthanized when ascites became visible, implantation of the gastric cancer cells was confirmed in all of the euthanized mice. No cancer cell was found in one mouse (ZD6474 100 mg/kg/day, 44As3 implanted), and it was excluded from the analysis. The experimental animal protocols were approved by the Committee for Ethics of Animal Experimentation, and the experiments were conducted in accordance with the Guidelines for Animal Experiments of the National Cancer Center.

Oligonucleotide microarray study

A DNA microarray procedure was used to prepare the *in vitro* transcription products, and oligonucleotide array hybridization and scanning were carried out according to the Affymetrix protocols (Santa Clara, CA). In brief, total RNA extracted from the tumor samples was analyzed with the Agilent 2100 Bioanalyzer (Agilent Technologies, Waldbronn, Germany) and cRNA was synthesized with the GeneChip® 3′-Amplification Reagents One-Cycle cDNA Synthesis Kit (Affymetrix). The cRNA were then labeled and purified for use as probes. Hybridization was carried out to the Affymetrix GeneChip HG-U133 Plus2.0 array for 16 hr at 45°C. After washing the glass slides, spot intensity was measured by scanning with a GeneChip® Scanner3000 (Affymetrix) and converted to numerical data with GeneChip Operating Software, Ver.1 (Affymetrix).

Six GeneChips were used to primary implanted 58as1 tumor samples from the vehicle control group ($n = 2$), and the ZD6474-treated group ($n = 2$, 50 mg/kg group; $n = 2$, the 100 mg/kg group).

Statistical analysis

All statistical calculations, except the analysis of the microarray data, were carried out using StatView version 5 software (SAS Institute Inc., Cary, NC). A p-value of <0.05 was considered significant. The microarray data were analyzed with GeneSpring software (Silicon Genetics, Redwood City, CA). The expression data were normalized across the sample set by the 50th percentile of each chip's intensity range. Relative expression data for each probe set were generated by median normalization. The fold change (mean value of the ZD6474-treatment group/mean value of the vehicle control group) was calculated, and genes with >2-fold change or <0.5-fold change were selected.

Results

Cell sensitivity to ZD6474 in vitro *and expression of VEGFR and EGFR*

Cell sensitivity to ZD6474 and the expression levels of EGFR, VEGFR and VEGF were examined in the 58As1 cells. The growth-inhibitory effect of ZD6474 and gefitinib was assessed by an MTT assay. The IC_{50} values of ZD6474 and gefitinib for 58As1 cells were 5.8 ± 1.8 and 11.0 ± 3.0 μM, respectively, suggesting that 58As1 cells are not sensitive to ZD6474 or gefitinib *in vitro*, compared to the "hypersensitive" PC-9 cells (IC_{50} values = 0.09 and 0.03 μM, respectively).[15] The 58As1 cells expressed a relatively high level of EGFR compared to the cells expressing high (PC-9) and low (HEK293) levels of EGFR, but the phosphorylation status was low (Fig. 1*a*). The expression levels of VEGFR and VEGF-A,C were measured by RT-PCR. A low

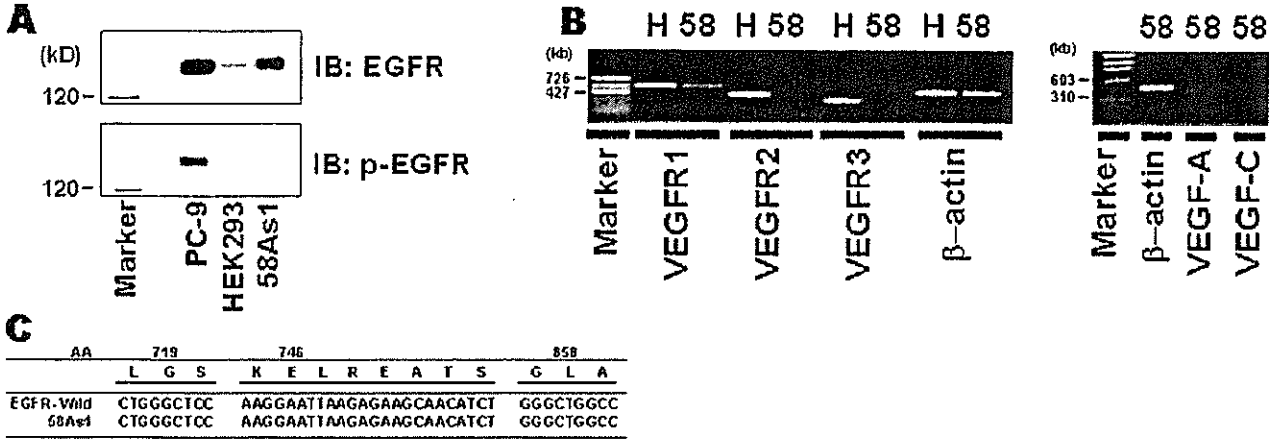

FIGURE 1 – Cellular characteristics of 58As1 cells. (*a*) EGFR expression and phosphorylation levels determined by Western blotting. A moderately high level of EGFR expression was observed in 58As1 cells, compared to cells expressing high (PC-9) and low (HEK293) levels of EGFR. The phosphorylation of EGFR status in 58As1 cells was low under normal culture conditions. IB, immunoblotting. Molecular marker: 120 kD. (*b*) Expression levels of VEGFR and VEGF-A and VEGF-C were measured by RT-PCR. A low level of VEGFR1 expression was detected in 58As1 cells, but no expression of VEGFR-2 or 3 was detected. 58As1 cells expressed VEGF-A but not VEGF-C. H, human umbilical vein endothelial cells. 58: 58As1. (*c*) EGFR sequence in 58As1 cells. No mutations were detected near the ATP-binding domains in 58As1 cells. AA, amino acid.

level of VEGFR1 expression was found in the 58As1 cells, but no VEGFR2 or VEGFR3 expression was detected. The 58As1 cells expressed VEGF-A, but not VEGF-C (Fig. 1*b*). Our results suggest that the lymphatic-metastasis-related VEGF-C and VEGFR3 are not involved in the inhibitory effect of ZD6474 on tumor dissemination observed in our present study *in vivo*.

Because EGFR mutations may be a determinant of tumor cell sensitivity to ZD6474,[15] exons 18–21 of EGFR mRNA from 58As1 cells were sequenced. No mutations near the ATP-binding domains[18,19] were detected, the 58As1 cells were concluded to express the wild-type EGFR.

Growth-inhibitory effect of ZD6474 in the orthotopic model in vivo

To examine the antitumor effect of ZD6474 on gastric cancer, we assessed the growth-inhibitory effect of ZD6474 by measuring implanted tumor volume after 14 days of p.o. treatment *in vivo*. A significant growth-inhibitory effect was observed in the ZD6474 (100 mg/kg/day) group in comparison with the vehicle control group ($p = 0.027$) in athymic mice implanted with 58As1 cells (Fig. 2*a*). Average tumor volume in the vehicle control group, 50 mg/kg/day ZD6474 group and 100 mg/kg/day ZD6474 groups was 106.3 ± 81.8 mm^3, 79.9 ± 70.0 mm^3, and 42.3 ± 24.8 mm^3, respectively.

Histological examination of H&E stained specimens showed a marked reduction in the number of cancer cells in the sub-mucosal lesions and the presence of necrotic tissue in the ZD6474 groups (Fig. 2*b*), suggesting that ZD6474 inhibits the growth of primary gastric tumor *in vivo*.

Inhibitory-effect of ZD6474 on peritoneal dissemination

To monitor the inhibitory effect of ZD6474 on peritoneally disseminated human cancer cells, the mRNA expression ratio of human β-actin/murine β-actin was measured with appropriate specific primers in cells collected from intraperitoneal lavage fluid. A significantly lower level of human-derived β-actin was observed in the 100 mg/kg/day ZD6474 group than in the vehicle control group ($p = 0.049$) (Fig. 2*c,d*), indicating that ZD6474 inhibits the intraperitoneal dissemination of gastric cancer in a dose-dependent manner.

Effect of ZD6474 on survival

In the survival experiment, we examined the effect of ZD6474 (p.o. or i.p.) on the survival of mice implanted with 58As1 or 44As3 cells. Both p.o. and i.p. administration of ZD6474 50 mg/kg/day significantly improved the survival of 44As3-implanted mice ($p = 0.0009$, $p = 0004$ *vs.* control, Fig. 3*b*), but did not significantly improve the survival of 58As1-implanted mice ($p = 0.09$, $p = 0.4$ *vs.* control, Fig. 3*a*). The median survival time of the 58As1-implanted mice was 33 days in the control group, 40 days in the i.p. group, and 46 days in the *p.o.* group, whereas in the 44As3-implanted mice, it was 34 days, 43 days and 53 days, respectively. Oral administration of ZD6474 was more effective than i.p. injection ($p = 0.049$) in the 44As3-implanted mice (Fig. 3*b*). These results suggest that ZD6474 is an active against gastric cancer.

Regulation of the gene expression by ZD6474 in vivo

To identify putative tumor biomarkers that reflect the efficacy of ZD6474 in vivo, we analyzed the gene expression profiles of implanted-tumor samples with oligonucleotide microarray. Expression of 26 genes was upregulated by 2-fold or more in the ZD6474 treatment group compared to the control group, whereas 2 genes were downregulated (Fig. 4*a*). Interestingly, of 26 upregulated genes, 9 of these genes were reported previously to be hypoxia-inducible: *IGFBP3* (*insulin-like growth factor binding protein 3*), *ADM* (*adrenomedullin*), *ANGPTL4* (*angiopoietin-like 4*), *PLOD2* (*procollagen-lysine, 2-oxoglutarate 5-dioxygenase 2*), *DSIPI* (*delta sleep inducing peptide, immunoreactor*), *ENO2* (*enolase 2*), *NDRG1* (*N-myc downstream regulated gene 1*) *HIG2* (*hypoxia-inducible protein 2*) and *BNIP3L* (*BCL2/adenovirus E1B 19 kDa interacting protein 3-like*). To confirm upregulation of the genes, we measured the expression levels of representative genes, *IGFBP3* and *ADM*, by RT-PCR in murine tumor samples (Fig. 4*b*).

Discussion

A correlation between somatic EGFR mutations in non-small cell lung cancer cells and sensitivity to EGFR-specific tyrosine kinase inhibitors, including gefitinib and erlotinib, has been demonstrated recently,[18–20] and a similar observation was made in regard to ZD6474 *in vitro*.[15] We demonstrated previously that cells transfected with mutated EGFR were ~60-fold more sensitive to ZD6474 *in vitro*. EGFR tyrosine kinase inhibitors may pro

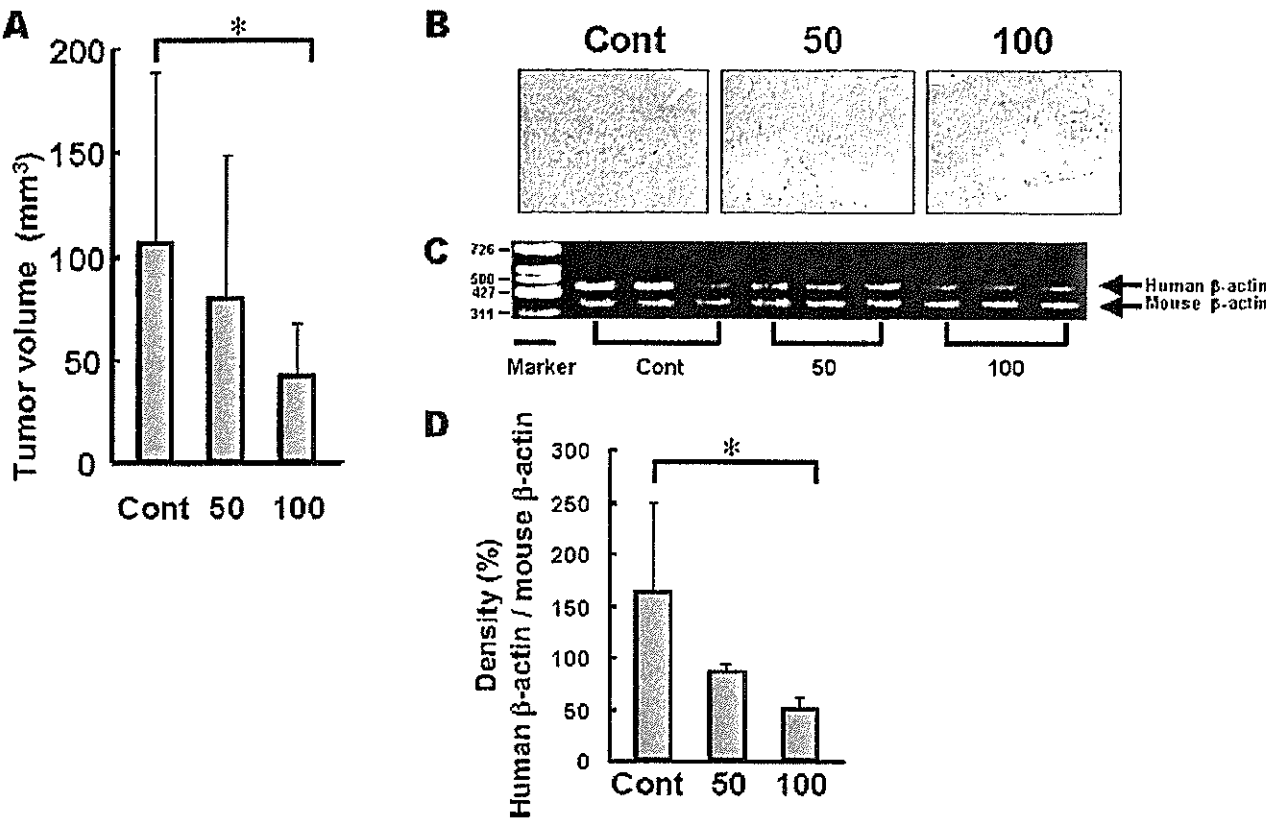

FIGURE 2 – Antitumor effect of ZD6474 in an orthotopic dissemination model *in vivo*. (*a*) *In vivo* growth-inhibitory effect of ZD6474. The implanted tumor volume was calculated after 14 days of treatment (p.o.). *Athymic mice (n = 7) per group were implanted with 58As1 cells, and a significant growth inhibitory effect was observed in the 100 mg/kg/day group, compared to the vehicle control group (p = 0.027). (*b*) Representative HE staining of tumor tissue in mice treated with ZD6474. The number of cancer cells in the sub-mucosal lesions was clearly lower and necrotic tissue was visible in the ZD6474 group, compared to the control group. (*c*) Disseminated cancer cells were collected from intraperitoneal lavage fluid to measure the ratio of tumor-derived human β-actin to murine β-actin using RT-PCR and specific primers (3 mice/group). Total RNA was equalized to 5 μg for each sample. (*d*) Densitometric analysis. Ratio of β-actin levels. *Significantly lower level of human-derived β-actin was detected in the 100 mg/kg/day ZD6474 group than in the control group (p = 0.049). The data shown are means ± SD. Cont, vehicle control; 50, ZD6474 50 mg/kg/day group; 100, ZD6474 100 mg/kg/day group. Significance was analyzed by Student's t-test.

vide particularly effective therapy for the subset of lung cancer patients whose tumor cell growth is highly dependent on EGFR signaling, including patients with tumor cells harboring activated, mutated EGFR. The proportion of patients with tumors highly dependent on EGFR signaling may be relatively small among various cancer patient populations. Therefore, additional treatment options for patients with cancers less dependent on EGFR signaling are also needed. It was concluded that 58As1 cells expressing wild-type EGFR are not highly dependent on EGFR signaling *in vitro* because the IC_{50} for growth inhibition by ZD6474 (5.8 μM) fell within the range of sensitivity reported by others for tumor cells *in vitro* (2.7–13.5 μM)[10] and because the IC_{50} for growth inhibition by gefitinib, a highly selective EGFR tyrosine kinase inhibitor, was >10μM. As a result, the concentration of ZD6474 required to inhibit 58As1 cell growth *in vitro* was 97-fold greater than required to inhibit VEGF-dependent HUVEC proliferation.[10] Nonetheless, ZD6474 significantly inhibited 58As1 tumor growth *in vivo* (Fig. 2*a*), suggesting that ZD6474 is active against gastric cancers expressing wild-type EGFR *in vivo* and that ZD6474 inhibition of tumor angiogenesis is likely to contribute significantly to this antitumor effect.

Our present study is unique because our aggressive and spontaneous intraperitoneal-dissemination model is considered a very good model of tumor progression in gastric cancer patients clinically, especially of the undifferentiated-type. Indeed, Paclitaxel and CPT-11 have been demonstrated to exhibit a growth-inhibitory effect and survival benefit in this model,[17] but gefitinib did not in preliminary result (data not shown). The positive results with ZD6474 in our present study suggest that this agent may be clinically useful in gastric cancer. We had hypothesized that direct intraperitoneal injection of ZD6474 is more effective than oral administration to inhibit intraperitoneal dissemination and result in better survival, however, the result showed that oral administration led to better survival in 44As3-inplanted mice (Fig. 3*b*).

ZD6474 inhibited the intraperitoneal dissemination of gastric cancer cells in our dissemination model. Although the mechanisms underlying this effect remain unclear, a few possibilities can be speculated: based on clinical evidence, the depth of tumor invasion and clinical staging is thought to be closely related to peritoneal dissemination.[21] Thus, one possible mechanism of the reduction of intraperitoneal dissemination may have resulted from a reduction in the serosal penetration of the cancer cells by "antitumor effect of ZD6474" on the implanted tumors. Although it is unclear whether ZD6474 has an inhibitory effect against distal metastasis to the liver and lymph nodes, for examples, it is not surprising that ZD6474 inhibits "intraperitoneal dissemination." Evaluation of its effect on distal metastasis will be the subject of a future investigation in our laboratory. Small tumor lesions (up to 2 mm) may obtain the oxygen and nutrients

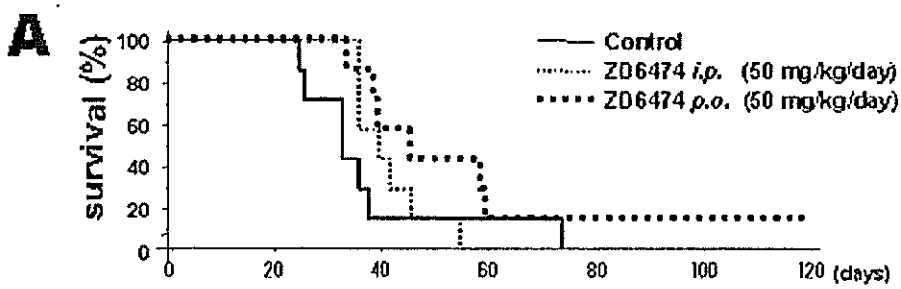

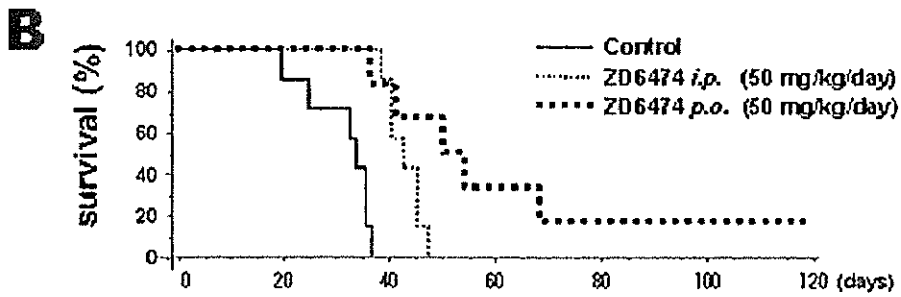

FIGURE 3 Survival curve of 58As1 cells- (*a*) and 44As3 cells- (*b*) implanted mice treated with ZD6474. Both p.o. and i.p. administration of ZD6474 50 mg/kg/day significantly improved the survival of 44As3-implanted mice ($p = 0.0009$, $p = 0004$ *vs.* control), but did not significantly improve the survival of mice implanted with 58As1 cells ($p = 0.09$, $p = 0.4$ *vs.* control). The p values were calculated by the log-rank test.

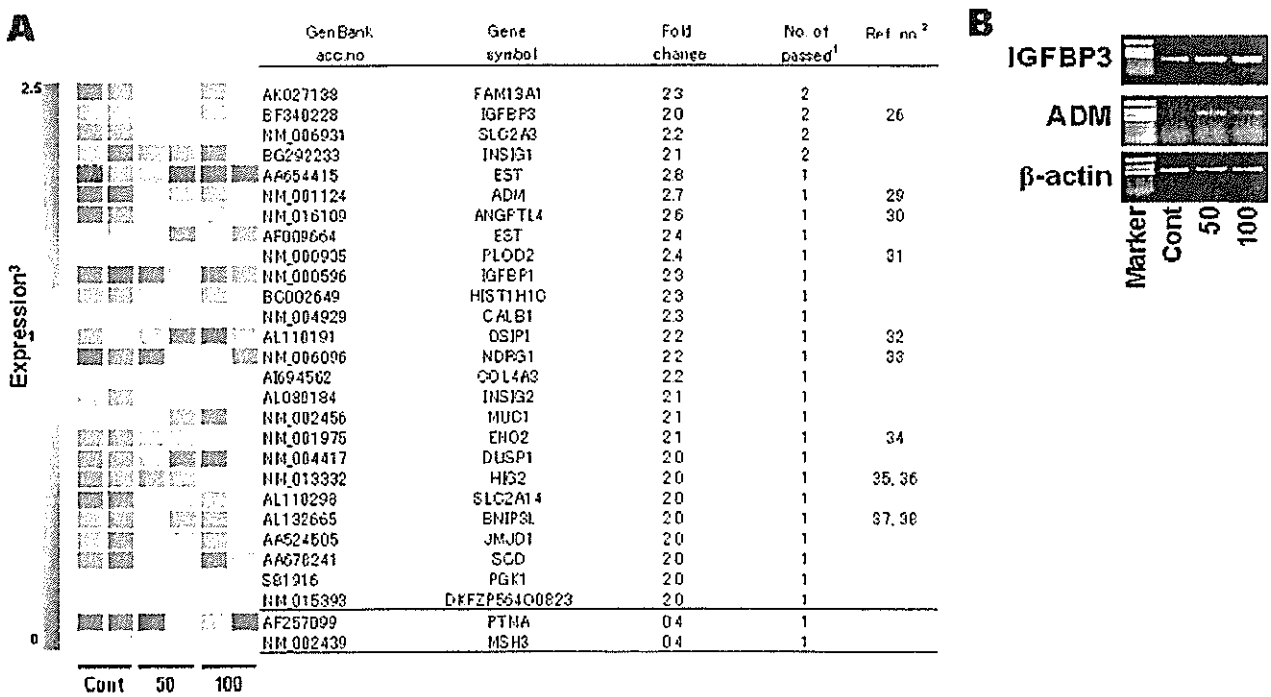

GenBank acc.no	Gene symbol	Fold change	No. of passed[1]	Ref. no.[2]
AK027138	FAM13A1	23	2	
BF340228	IGFBP3	20	2	26
NM_006931	SLC2A3	22	2	
BG292233	INSIG1	21	2	
AA654415	EST	28	1	
NM_001124	ADM	27	1	29
NM_016109	ANGPTL4	26	1	30
AF009664	EST	24	1	
NM_000935	PLOD2	24	1	31
NM_000596	IGFBP1	23	1	
BC002649	HIST1H1C	23	1	
NM_004929	CALB1	23	1	
AL110191	OSIP1	22	1	32
NM_006096	NDRG1	22	1	33
AI694502	COL4A3	22	1	
AL080184	INSIG2	21	1	
NM_002456	MUC1	21	1	
NM_001975	ENO2	21	1	34
NM_004417	DUSP1	20	1	
NM_013332	HIG2	20	1	35, 36
AL110298	SLC2A14	20	1	
AL132665	BNIP3L	20	1	37, 38
AA524505	JMJD1	20	1	
AA670241	SCD	20	1	
S81916	PGK1	20	1	
NM_015393	DKFZP564O0823	20	1	
AF257099	PTMA	04	1	
NM_002439	MSH3	04	1	

FIGURE 4 Candidate genes for biomarkers regulated by ZD6474 treatment. Each colored block represents the expression level of a given gene in an individual sample. (*a*) Upregulated genes with a >2-fold change or <0.5-fold change are shown (mean value in the ZD6474 group/vehicle control group). Cont, vehicle control group, $n = 2$; 50, ZD6474 50 mg/kg/day group, $n = 2$; 100, ZD6474 100 mg/kg/day group, $n = 2$. [1]Number of different probes that passed fold-change criteria above. [2]Reference number for genes whose expression has been reported to be related to hypoxia. [3]Red represents increased expression and blue represents decreased expression relative to the normalized expression of the gene across all samples. (*b*) mRNA expression levels of 2 representative genes, *IGFBP-3* and *ADM*, detected by RT-PCR in tumors treated with ZD6474. *IGFBP-3* and *ADM* mRNA expression was induced in response to ZD6474.

they need by passive diffusion, but angiogenesis is required for the growth of tumors larger than 2 mm.[22] A second possible mechanism is that ZD6474 may inhibit the growth or migration of tumor vascular endothelial cells in "small tumor lesions" by inhibiting VEGFR2-dependent intracellular signaling. This effect would be expected to limit metastatic tumor growth due to lack of oxygen and nutrients, and reduce the dissemination of cancer cells.

To identify putative biomarkers of the pharmacodynamic effects of ZD6474 *in vivo*, we identified 28 candidate genes from implanted 58As1 tumor samples by oligonucleotide microarray analysis (Fig. 4*a*). IGFBP-3 has multiple functions, including in the induction of apoptosis,[23] the inhibition of cancer cell proliferation,[24] and carcinogenesis[25] and IGFBP-3 expression is transcriptionally upregulated under hypoxic conditions.[26] A recent study has also shown that EGFR regulates IGFBP-3 expression and secretion.[27] The inhibitory effect of ZD6474 on EGFR kinase may be associated with the upregulation of IGFBP-3. ADM, which was first identified in a human pheochromocytoma, is known to regulate circulation by acting as a hormone.[28] Adrenomedullin is also induced by hypoxia and may have a role in protecting against hypoxic cellular damage in human retinal pigment epithelial cells.[29] Expressions of nine of the upregulated genes, *IGFBP-3*, *ADM*, *ANGPTL4*, *PLOD2*, *DSIPI*, *NDRG1*, *ENO2*, *HIG2* and *BNIP3L*, has been reported previously to be induced by hypoxia.[26,29–38] We hypothesize that ZD6474 inhibits neovascularization in tumors, thereby limiting the oxygen and nutrient supply and resulting in tumor hypoxia and upregulation of hypoxia-inducible genes. If this hypothesis is correct, hypoxia-regulated genes and gene products might be useful biomarkers for the pharmacodynamic effects of ZD6474 and other anti-angiogenic agents in preclinical and clinical settings. We are now investigating whether these genes and gene products can be used as biomarkers for the efficacy of ZD6474 in a correlative study.

Future directions of our study include: (*i*) to compare the antitumor effect of other "anti-vascular agents" with ZD6474 in this model; (*ii*) to evaluate combination therapy with ZD6474 plus anticancer agents; (*iii*) to evaluate the antitumor effect of ZD6474 against micro-metastasis *in vivo*; and (*iv*) to confirm the usefulness of the 9 candidate genes as biomarkers in clinically.

In conclusion, we demonstrated that ZD6474 inhibited tumor growth, suppressed intraperitoneal dissemination, and prolonged survival in a highly metastatic orthotopic gastric cancer model. We carried out a microarray analysis of tumor samples and we identified 9 hypoxia-inducible genes as candidate biomarkers for monitoring the effects of ZD6474 therapy. These findings provide a strong preclinical rationale for investigating ZD6474 for the treatment of gastric cancer in the clinic.

Acknowledgements

Grants were received from the 3rd-Term Comprehensive 10-Year Strategy for Cancer Control and from a Grant-in-Aid for Scientific Research from the Ministry of Education, Culture, Sports, Science and Technology of Japan (Grant number: 12217165). T.A. is the Recipient of a Research Resident Fellowship from the Foundation of Promotion of Cancer Research in Japan.

References

1. Vanhoefer U, Rougier P, Wilke H, Ducreux MP, Lacave AJ, Van Cutsem E, Planker M, Santos JG, Piedbois P, Paillot B, Bodenstein H, Schmoll HJ, et al. Final results of a randomized phase III trial of sequential high-dose methotrexate, fluorouracil, and doxorubicin versus etoposide, leucovorin, and fluorouracil versus infusional fluorouracil and cisplatin in advanced gastric cancer: A trial of the European Organization for Research and Treatment of Cancer Gastrointestinal Tract Cancer Cooperative Group. J Clin Oncol 2000;18:2648–57.
2. Ohtsu A, Shimada Y, Shirao K, Boku N, Hyodo I, Saito H, Yamamichi N, Miyata Y, Ikeda N, Yamamoto S, Fukuda H, Yoshida S. Randomized phase III trial of fluorouracil alone versus fluorouracil plus cisplatin versus uracil and tegafur plus mitomycin in patients with unresectable, advanced gastric cancer: the Japan Clinical Oncology Group Study (JCOG9205). J Clin Oncol 2003;21:54–9.
3. Moriguchi S, Kamakura T, Odaka T, Nose Y, Maehara Y, Korenaga D, Sugimachi K. Clinical features of the differentiated and undifferentiated types of advanced gastric carcinoma: univariate and multivariate analyses. J Surg Oncol 1991;48:202–6.
4. Ferrara N, Davis-Smyth T. The biology of vascular endothelial growth factor. Endocr Rev 1997;18:4–25.
5. Nicosia RF. What is the role of vascular endothelial growth factor-related molecules in tumor angiogenesis? Am J Pathol 1998;153:11–6.
6. Mustonen T, Alitalo K. Endothelial receptor tyrosine kinases involved in angiogenesis. J Cell Biol 1995;129:895–8.
7. Shibuya M. Vascular endothelial growth factor receptor-2: its unique signaling and specific ligand, VEGF-E. Cancer Sci 2003;94:751–6.
8. Manley PW, Bold G, Brueggen J, Fendrich G, Furet P, Mestan J, Schnell C, Stolz B, Meyer T, Meyhack B, Stark W, Strauss A, et al. Advances in the structural biology, design and clinical development of VEGF-R kinase inhibitors for the treatment of angiogenesis. Biochim Biophys Acta 2004;1697:17–27.
9. Hurwitz H, Fehrenbacher L, Novotny W, Cartwright T, Hainsworth J, Heim W, Berlin J, Baron A, Griffing S, Holmgren E, Ferrara N, Fyfe G, et al. Bevacizumab plus irinotecan, fluorouracil, and leucovorin for metastatic colorectal cancer. N Engl J Med 2004;350:2335–42.
10. Wedge SR, Ogilvie DJ, Dukes M, Kendrew J, Chester R, Jackson JA, Boffey SJ, Valentine PJ, Curwen JO, Musgrove HL, Graham GA, Hughes GD, et al. ZD6474 inhibits vascular endothelial growth factor signaling, angiogenesis, and tumor growth following oral administration. Cancer Res 2002;62:4645–55.
11. Ciardiello F, Caputo R, Damiano V, Troiani T, Vitagliano D, Carlomagno F, Veneziani BM, Fontanini G, Bianco AR, Tortora G. Antitumor effects of ZD6474, a small molecule vascular endothelial growth factor receptor tyrosine kinase inhibitor, with additional activity against epidermal growth factor receptor tyrosine kinase. Clin Cancer Res 2003;9:1546–56.
12. Sandstrom M, Johansson M, Andersson U, Bergh A, Bergenheim AT, Henriksson R. The tyrosine kinase inhibitor ZD6474 inhibits tumour growth in an intracerebral rat glioma model. Br J Cancer 2004;91:1174–80.
13. McCarty MF, Wey J, Stoeltzing O, Liu W, Fan F, Bucana C, Mansfield PF, Ryan AJ, Ellis LM. ZD6474, a vascular endothelial growth factor receptor tyrosine kinase inhibitor with additional activity against epidermal growth factor receptor tyrosine kinase, inhibits orthotopic growth and angiogenesis of gastric cancer. Mol Cancer Ther 2004;3:1041–8.
14. Taguchi F, Koh Y, Koizumi F, Tamura T, Saijo N, Nishio K. Anticancer effects of ZD6474, a VEGF receptor tyrosine kinase inhibitor, in gefitinib (Iressa) sensitive and resistant xenograft models. Cancer Sci 2004;95:984–9.
15. Arao T, Fukumoto F, Takeda M, Tamura T, Saijo N, Nishio K. Small in-frame deletion in the epidermal growth factor receptor as a target for ZD6474. Cancer Res 2004;64:9101–4.
16. Yanagihara K, Tanaka H, Takigahira M, Ino Y, Yamaguchi Y, Toge T, Sugano K, Hirohashi S. Establishment of two cell lines from human gastric scirrhous carcinoma that possess the potential to metastasize spontaneously in nude mice. Cancer Sci 2004;95:575–82.
17. Yanagihara K, Takigahira M, Tanaka H, Komatsu T, Fukumoto H, Koizumi F, Nishio K, Ochiya T, Ino Y, Hirohashi S. Development and biological analysis of peritoneal metastasis mouse models for human scirrhous stomach cancer. Cancer Sci 2005;6:323–32.
18. Lynch TJ, Bell DW, Sordella R, Gurubhagavatula S, Okimoto RA, Brannigan BW, Harris PL, Haserlat SM, Supko JG, Haluska FG, Louis DN, Christiani DC, et al. Activating mutations in the epidermal growth factor receptor underlying responsiveness of non-small-cell lung cancer to gefitinib. N Engl J Med 2004;350:2129–39.
19. Paez JG, Janne PA, Lee JC, Tracy S, Greulich H, Gabriel S, Herman P, Kaye FJ, Lindeman N, Boggon TJ, Naoki K, Sasaki H, et al. EGFR mutations in lung cancer: correlation with clinical response to gefitinib therapy. Science 2004;304:1497–500.
20. Pao W, Miller V, Zakowski M, Doherty J, Politi K, Sarkaria I, Singh B, Heelan R, Rusch V, Fulton L, Mardis E, Kupfer D, et al. EGF receptor gene mutations are common in lung cancers from "never smokers" and are associated with sensitivity of tumors to gefitinib and erlotinib. Proc Natl Acad Sci USA 2004;101:13306–11.
21. Yang SH, Lin JK, Lai CR, Chen CC, Li AF, Liang WY, Jiang JK. Risk factors for peritoneal dissemination of colorectal cancer. J Surg Oncol 2004;87:167–73.
22. Folkman J. What is the evidence that tumors are angiogenesis dependent? J Natl Cancer Inst 1990;82:4–6.
23. Kim HS, Ingermann AR, Tsubaki J, Twigg SM, Walker GE, Oh Y. Insulin-like growth factor-binding protein 3 induces caspase-dependent apoptosis through a death receptor-mediated pathway in MCF-7 human breast cancer cells. Cancer Res 2004;64:2229–37.
24. Kinman L, Powolny-Budnicka I, Sylla P, Whelan RL. Insulin-like growth factor-binding protein 3 inhibits growth of experimental colorectal carcinoma. Surgery 2004;136:205–9.

25. Renehan AG, Zwahlen M, Minder C, O'Dwyer ST, Shalet SM, Egger M. Insulin-like growth factor (IGF)-I, IGF binding protein-3, and cancer risk: systematic review and meta-regression analysis. Lancet 2004;363:1346–53.
26. Koong AC, Denko NC, Hudson KM, Schindler C, Swiersz L, Koch C, Evans S, Ibrahim H, Le QT, Terris DJ, Giaccia AJ. Candidate genes for the hypoxic tumor phenotype. Cancer Res 2000;60: 883–7.
27. Takaoka M, Harada H, Andl CD, Oyama K, Naomoto Y, Dempsey KL, Klein-Szanto AJ, El-Deiry WS, Grimberg A, Nakagawa H. Epidermal growth factor receptor regulates aberrant expression of insulin-like growth factor-binding protein 3. Cancer Res 2004;64:7711–23.
28. Hirata Y, Hayakawa H, Suzuki Y, Suzuki E, Ikenouchi H, Kohmoto O, Kimura K, Kitamura K, Eto T, Kangawa K. Mechanisms of adrenomedullin-induced vasodilation in the rat kidney. Hypertension 1995;25:790–5.
29. Udono T, Takahashi K, Nakayama M, Yoshinoya A, Totsune K, Murakami O, Durlu YK, Tamai M, Shibahara S. Induction of adrenomedullin by hypoxia in cultured retinal pigment epithelial cells. Invest Ophthalmol Vis Sci 2001;42:1080–6.
30. Le Jan S, Amy C, Cazes A, Monnot C, Lamande N, Favier J, Philippe J, Sibony M, Gasc JM, Corvol P, Germain S. Angiopoietin-like 4 is a proangiogenic factor produced during ischemia and in conventional renal cell carcinoma. Am J Pathol 2003;162:1521–8.
31. Holbauer KH, Gess B, Lohaus C, Meyer HE, Katschinski D, Kurtz A. Oxygen tension regulates the expression of a group of procollagen hydroxylases. Eur J Biochem 2003;270:4515–22.
32. Khvatova EM, Samartzev VN, Zagoskin PP, Prudchenko IA, Mikhaleva II. Delta sleep inducing peptide (DSIP): effect on respiration activity in rat brain mitochondria and stress protective potency under experimental hypoxia. Peptides 2003;24:307–11.
33. Cangul H. Hypoxia upregulates the expression of the NDRG1 gene leading to its overexpression in various human cancers. BMC Genet 2004;5:27
34. Szturmowicz M, Burakowski J, Tomkowski W, Sakowicz A, Filipecki S. Neuron-specific enolase in non-neoplastic lung diseases, a marker of hypoxemia? Int J Biol Markers 1998;13:150–3.
35. Denko N, Schindler C, Koong A, Laderoute K, Green C, Giaccia A. Epigenetic regulation of gene expression in cervical cancer cells by the tumor microenvironment. Clin Cancer Res 2000;6:480–7.
36. Kenny PA, Enver T, Ashworth A. Receptor and secreted targets of Wnt-1/beta-catenin signalling in mouse mammary epithelial cells. BMC Cancer 2005;5:3.
37. Fei P, Wang W, Kim SH, Wang S, Burns TF, Sax JK, Buzzai M, Dicker DT, McKenna WG, Bernhard EJ, El-Deiry WS. Bnip3L is induced by p53 under hypoxia, and its knockdown promotes tumor growth. Cancer Cell 2004;6:597–609.
38. Sowter HM, Ratcliffe PJ, Watson P, Greenberg AH, Harris AL. HIF-1-dependent regulation of hypoxic induction of the cell death factors BNIP3 and NIX in human tumors. Cancer Res 2001;61: 6669–73.

Acta Med Kinki Univ Vol. 31, No. 2, 57 62, 2006

Progress in the field of molecular biology and application of biotechnology to medical oncology

Kazuto Nishio and Tokuzo Arao

Department of Genome Biology, Kinki University School of Medicine, Osakasayama, Osaka 589-8511, Japan

Abstract

Recent progress in the field of molecular biology has been expected to contribute to progress in the field of clinical medicine. Personalized medicine could be achieved by pharmacogenomics. Prospective clinical studies using biomarkers are considered to be important. Investigators should plan the study design and carefully perform such studies.

Key words: Pharmacogenomics, DNA chip, biomarker, prediction

Introduction

Remarkable progress has been made in the field of molecular biology in the 20th century (Table 1). The entire human genome has been sequenced by the Human Genome Project. The 21st century is, therefore, called the "Post Genome" era and further advances in the clinical application of biotechnology are expected. Applied biotechnology is also useful for both diagnostic and therapeutic oncology. Here, we shall discuss the application of biotechnology to the field of medical oncology.

Table 1 Progress in the field of molecular biology during the 20th century

year	event
1890	Mendelism
1926	Genes on chromosome (Mogan)
1944	DNA as gene component (Fibree)
1953	Double helix of DNA (Watson & Crick)
1956	Replication enzyme of DNA (Komburg)
1973	Recombination technology (Cohen)
1985	PCR (Mullis)
1990	Start the Human Genome Project
1998	Deciphering the human genome proceed to multicellular organism
2001	Decoding of the human genome by Celera Genomics Co.

Tissue Banking

Genome biology is expected to be applied to drug development. Drug development, such as that of cytotoxic anticancer drugs and molecular target drugs in the field of oncology, is one of the most upcoming fields. The first and most important step of drug screening is target identification and the search for seeds. The next step is screening of the compounds, followed by preclinical and clinical studies. It is considered that genomic information effectively contributes to the target identification and its validation. To obtain data about the human genome, analysis of human materials is essential. This approach is called the "Reverse Translational Research". In the clinical setting, it is also called "Molecular Correlative Study". These approaches are adopted by government-supported projects both in Japan and abroad. Pharmaceutical companies also aggressively conduct a search for seeds. Mega-pharmas, in particular, have already established the banking system for human materials. Japan has also started a banking system, but it seems to be still immature and Japan still falls behind other countries. The process of collecting clinical samples is called "Tissue Banking" or simply "Banking".

Pharmacogenomics

The approach mentioned above is also applied in the clinical setting. One of the well-recognized approaches is "Personalized Medicine,"

that allows therapy to be customized to individuals by analyzing the individual's genome. Analysis of the genome is called "pharmacogenomics" when it is related to treatment with drugs. "Pharmacogenomics" is a word combining "genomics" and "pharmacology". Broadly, pharamcogenomics includes the analysis of gene products, such as RNA and proteins. The pharmacogenomic approach is considered to contribute to health and welfare. The US and other governments are encouraging this strategy. For example, the US government provides guidance to the industry on the process of Investigational New Drug (IND), New Drug Application (NDA), and Biologic Licence Application (BLA). In our country, the Ministry of Health, Welfare, and Labour has requested for genomic information obtained by the genomic testing in clinical studies for pharmaceutical companies.

Application of pharamcogenomics is expected in three major stages: discovery, preclinical, and clinical stages (Table 2). Three examples are provided as follows; i) research on gene-related diseases; ii) relationship between gene polymorphism and response to drug treatment; iii) genomic tests for the prediction of drug responses. Examples 2 and 3 are considered to be closely associated with cancer treatment and will directly contribute to the exclusion of patients with severe toxicities or to the selection of responders and non-responders to a particular treatment. The markers obtained by pharmacogenomics are called as "biomarkers".

Biomarkers for molecule-targeting drugs

We would like to consider biomarkers for target-based drugs. 1) Overexpression of the target molecule; this is often detected by immunohistochemical analysis. Amplification of target molecules is detected by FISH, CISH or PCR. Somatic mutations in tumor tissues are detected by direct sequencing or other PCR-based assays. For the purification of tumor tissues, the microdissection technique is useful. There are biomarkers for conventional cytotoxic drugs. ERCC1 is an enzyme involved in DNA repair and its transcript levels have been reported to be related to the responses to platinum-containing regimens (e.g., cisplatin plus gemicitabine) in non-small cell lung cancer patients[1]. Thus, biomarkers could be determinants for predicting the sensitivity and responses of tumors to cytotoxic drugs.

As mentioned above, the EGFR somatic mutation in lung cancer is a hot topic. Strong correlation has been observed between EGFR somatic mutations and clinical responses to an EGFR-specific tyrosine kinase inhibitor, gefitinib. Thus, the EGFR mutation is a definite biomarker, and other somatic mutations of oncogenes in tumors have been also reported. These mutations could be used as new biomarkers to clarify subpopulations of patients that would respond to molecule-targeting drugs. Currently, trials for new molecule-targeting therapeutics are now underway for solid tumors. Treatment with angiogenesis inhibitors and antibodies are expected to improve the outcome of patients. New biomarkers need to be continually sought for this type of therapeutics.

Now, these molecular correlative studies are called as "Critical Path Research" in the field of drug development (Fig. 1).

Considering the background of aggressiveness of biomarker research, the average response to drugs is much lower than that of other diseases (Fig. 2).

The average response rate to anticancer drugs is 20-30%, which is inadequate. In order to improve the response rate to anticancer drugs, selection of subpopulations of patients that

Table 2 Three broad applications of pharmacogenomics

Discovery
Target identification
Mechanisms of Action
Target differentiation
Biomarker identification
Preclinical Toxicology
Toxicogenomics
In vivo mechanism of action
Biomarker identification
Clinical
In vivo mechanism of action
Biomarker development and validation

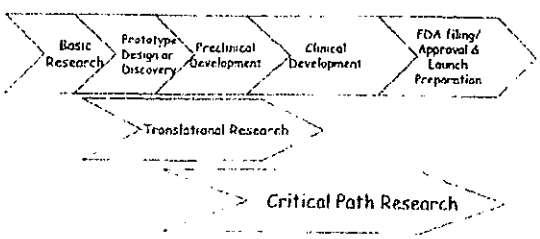

Fig. 1 Critical path. Significant benefit of bringing innovative products faster to the public

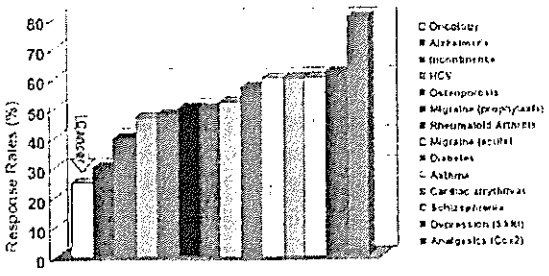

Fig. 2 The need for better predictive markers
(Paul Warning, Genentech, modified)

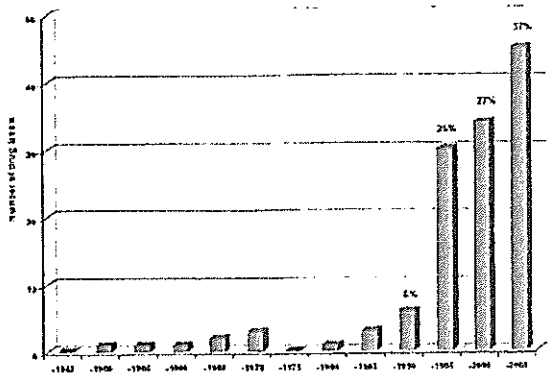

Fig. 3 Labels of approved drugs with pharmacogenomic information
(Fruch FW, CDER/FDA, modified)

would potentially show response is one strategy. At the same time, the labeling of drugs with pharmacogenomic data has been increasing recently (Fig. 3)

Government-related regulatory institutions in the US (Department of Health and Human Services, Food and Drug Administration, Center for Drug Evaluation and Research (CDER), Center for Biologic Evaluation and Research (CBER), Center for Devices and Radiological Health (CDRH)) developed a "Guideline for Industry," by which pharmaceutical companies are required to submit pharmacogenomic data. How should investigators assess/evaluate the data? Essentially, we should recognize three categories of pharmacogenomic information while selecting the treatment strategy: 1) test required, 2) test recommended, 3) information only.

Trastuzumab (Herceptin®) for breast cancer is a good example of the first; testing for anti-Her2 by FISH analysis (Herceptest®) is required for the administration of Trastuzumab. Although EGFR somatic mutation, EGFR immunohistochemistry, and FISH for FGFR are considered to be good biomarkers for predicting the response to EGFR-targeting drugs, they belong to the "Test only" category. It is not within the scope of this review to discuss why these differences exist. Anyway, applied pharmacogenomics is very important in the selection of appropriate subpopulations, and an increase in the number of "Test required" biomarkers is warranted.

Another point for discussion is that the pharmacogenomic approach has so far focused on the prediction or evaluation of adverse events. Single- nucleotide polymorphisms of metabolizing enzymes, such as p450 or UDP-glucuronoyltransferases (UGT)[2] are closely related to the toxicity profile of drugs. Therefore, tests for these genes are also included in the label of the drugs. The available evidence actually contributes to identify subpopulations of patients likely to show severe side effects. On the other hand, there is not much evidence, in terms of biomarkers, to distinguish accurately between responders and non-responders. It is important to consider the latter approach when considering personalized medicine.

Drug-diagnostic co-development

As mentioned before, the importance of pharmacogenomics has been discussed worldwide. Last year, the FDA proposed the new concept "drug-diagnostic co-development", although it is still in the draft stage and needs open discussion. What is the "co-development"? "Co-development" means: 1) Critical Path Research for biomarkers that would distinguish responders from non-responders in clinical studies; 2) research for avoiding severe toxicities; 3) clinical studies for POC (proof of concept) by monitoring pharmacodynamic markers. The endpoints of these approaches are to set the appropriate doses for each subpopulation or responders. Investigators should consider the study designs flexibly in these approaches. For example, randomized phase II studies and randomized discontinuation studies may be given more consideration. In addition, for the selection of biomarkers in Critical Path Research, more strict validation will be necessary, because the tests using the biomarkers will directly affect the treatment of each patient.

Problems in pharamcogenomics and future perspectives

Biomarker researches can be divided into two categories, "hypothesis-driven" and "hypothesis-free"; the former is to prove the power of preex-